

DIFFUSION BASED GAUSSIAN PROCESSES ON RESTRICTED DOMAINS

DAVID B DUNSON, HAU-TIENG WU, AND NAN WU

ABSTRACT. In nonparametric regression and spatial process modeling, it is common for the inputs to fall in a restricted subset of Euclidean space. For example, the locations at which spatial data are collected may be restricted to a narrow non-linear subset, such as near the edge of a lake. Typical kernel-based methods that do not take into account the intrinsic geometry of the domain across which observations are collected may produce sub-optimal results. In this article, we focus on solving this problem in the context of Gaussian process (GP) models, proposing a new class of diffusion-based GPs (DB-GPs), which learn a covariance that respects the geometry of the input domain. We use the term ‘diffusion-based’ as the idea is to measure intrinsic distances between inputs in a restricted domain via a diffusion process. As the heat kernel is intractable computationally, we approximate the covariance using finitely-many eigenpairs of the Graph Laplacian (GL). Our proposed algorithm has the same order of computational complexity as current GP algorithms using simple covariance kernels. We provide substantial theoretical support for the DB-GP methodology, and illustrate performance gains through toy examples, simulation studies, and applications to ecology data.

Key Words: Bayesian; Graph Laplacian; Heat kernel; Manifold; Nonparametric regression; Restricted domain; Semi-supervised; Spatial process modeling

1. INTRODUCTION

We are interested in problems in which data are collected on ‘inputs’ $x = (x_1, \dots, x_D) \in S \subset \mathbb{R}^D$ and ‘outputs’ $y \in \mathbb{R}$, with S a subset of \mathbb{R}^D . Labeled training data $\mathcal{D} = \{x_i, y_i\}_{i=1}^m$ are available for samples $i = 1, \dots, m$, along with (possibly) unlabeled data $\mathcal{U} = \{x_i\}_{i=m+1}^{m+n}$. There are several settings in which this problem arises, including (1) nonparametric regression focused on using features x to predict outcome y , (2) spatial process modeling in which x_i represents the spatial location of sample i and y_i is a measured variable at that location, and (3) computer model emulation in which x corresponds to an input into a computer model that is expensive to run and y corresponds to the output. Gaussian process (GP) models are routinely used in all these settings, but without explicitly taking into account the geometry of S or using the unlabeled data to improve estimation of the unknown input-output function. It is common in all three settings for S to be highly restricted and non-linear - in spatial process modeling, there may be geographic constraints on the locations in which you can collect information on y (e.g. y may be abundance of a species living in shallow aquatic environments), while in computer model emulation, inputs commonly need to satisfy some physical law that implies substantial restrictions.

For concreteness, we focus on the following model throughout the paper, while noting that many elaborations (e.g. to include other covariates in addition to spatial location in spatial process modeling) are straightforward within the framework we will propose,

$$(1) \quad y_i = f(x_i) + \eta_i, \quad \eta_i \sim N(0, \sigma_{noise}^2),$$

where $f : S \rightarrow \mathbb{R}$ is an unknown regression function that is assigned a GP prior centered at zero with covariance function $C(x, x')$ and σ_{noise}^2 is the measurement error variance (this can be set to zero for deterministic computer models). The choice of $C(x, x')$ has a fundamental impact on the results; in the above three application areas, the most common choices of covariance function are the squared exponential and its generalization, the Matérn. Both choices depend critically on the distance between inputs x and x' ; by far the most common choice in practice is the Euclidean distance.

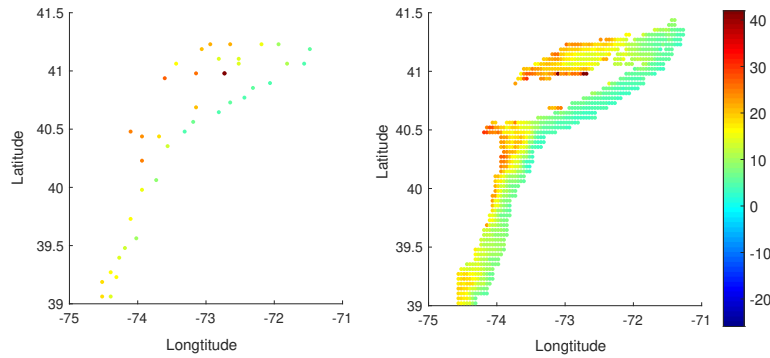


FIGURE 1. Each point corresponds to the log chlorophyll concentration at a single sampling location along the coastal region of Long Island. The left panel shows a subset of labeled data and the right panel shows all the data.

We use the following example to illustrate the problems with ignoring the geometry of S and simply using a Euclidean distance-based kernel. Fisheries biologists are interested in studying food supplies for juvenile fish living in shallow waters along the coast. With this goal in mind, we consider data on chlorophyll along the coastal region of Long Island at latitudes between $39^\circ N$ and $41.5^\circ N$ and longitudes between $71^\circ W$ and $75^\circ W$. In Figure 1, we plot the natural log of the chlorophyll concentration at each location; for illustration we hold out labels for a subset of the data points and show the labeled data in the left panel and all the data in the right panel. We fit a GP with Euclidean distance in the covariance to the above data, and show the predicted values in the left panel of Figure 2. There is a substantial change in chlorophyll concentration between the north side of Long Island around $72.6^\circ W$, $41^\circ N$ and the south side around $72.6^\circ W$, $40.7^\circ N$. When we use a GP with Euclidean distance in the covariance, there is inappropriate smoothing across the land between these locations, leading to poor predictions.

There have been attempts to solve related problems in the literature. [5] assumes S is an unknown submanifold in a Euclidean space and develops a locally linear regression method on the manifold. See the citations therein for other relevant work. Also see [26, 27, 2, 18, 11, 24] for semi-supervised learning approaches. An alternative strategy is to choose a covariance in a GP prior that respects the geometry of S , but it is not clear how to specify such a covariance. When the subset S is a submanifold in a Euclidean space, the heat kernel of S that characterizes the diffusion of heat flowing out of a point in S is a potentially appealing choice. [3] studies theoretical properties of the posterior distribution, such as rates of contraction, for related models. Unfortunately, the heat kernel is typically intractable to calculate. For known manifolds, [17] propose an extrinsic GP that embeds the manifold in a higher-dimensional Euclidean space, while [19] propose an intrinsic GP relying on a Monte Carlo (MC) approximation to the heat kernel. The intrinsic GP is only applicable to known manifolds and their MC approximation is very expensive computationally, relying on simulating Brownian motion many times and calculating proportions of paths from a starting point ending up close to a target point.

In this article, we develop a novel Diffusion-based GP (DB-GP) to solve the above problem with predictors on an unknown subset S of \mathbb{R}^D , which is not necessarily a manifold. The key idea is to construct a covariance that incorporates the intrinsic geometry of S . This is accomplished through taking *finitely* many eigenpairs of the graph Laplacian (GL) using the labeled and unlabeled predictor values. The GL is widely studied in spectral graph theory [6], and corresponds to the infinitesimal generator of a random walk on the sampled data points. The covariance in the DB-GP approximates a diffusion process on S with respect to intrinsic distances between data points. To provide a teaser illustrating practical advantages of the DB-GP, we fit our DB-GP to the dataset of the chlorophyll concentration

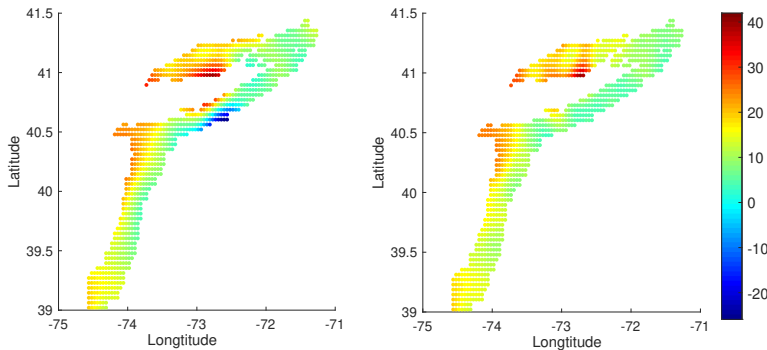


FIGURE 2. We fit GP models to predict held-out log chlorophyll concentration data shown in Figure 1. The left panel shows the results for a GP with squared exponential covariance, while the right panel shows the results for our DB-GP.

around Long Island. The predicted values are shown in the right panel of Figure 2. Tuning parameters in the covariance functions were estimated by maximizing marginal likelihoods [20].

The proposed DB-GP can be used broadly in place of existing GP models. The method is designed to adapt to the support of the sample points, and one does not need to know *a priori* that the data have constrained support. We find in practice that the DB-GP often outperforms GPs with standard off the shelf covariance functions in general applications. In addition to the novel DB-GP methodology, a major contribution of this paper is the theory we have developed in support of the DB-GP. We first associate the GL with an integral operator for any subset S of the Euclidean space. We discuss theoretical properties of the integral operator and define the covariance function of the DB-GP by using finitely many eigenpairs of the integral operator. When S is an embedded submanifold of \mathbb{R}^D , we provide the convergence rate of the DB-GP covariance matrix to the DB-GP covariance function. We show the stability of the GL (hence the DB-GP algorithm) when there are measurement errors so that predictors do not fall exactly within S . Finally, when S is an embedded submanifold of \mathbb{R}^D , we provide theory on contraction of the posterior for f around the true function f_0 under some regularity assumptions.

2. DIFFUSION BASED GAUSSIAN PROCESSES ON SUBSETS OF EUCLIDEAN SPACE

Focusing on equation (1), we propose a new approach for choosing the covariance function C in the Gaussian process; our proposed approach differs from current standard methods in not treating C as a pre-specified function having a small number of unknown parameters (e.g. squared exponential or Matérn) but instead estimates the covariance in a manner that takes into account the structure of the support S as well as information in both the labeled and unlabeled data. Before introducing the proposed covariance, we provide a review of prediction based on GPs.

2.1. Gaussian process review. Denote $\mathbf{f} \in \mathbb{R}^m$ to be the discretization of f over x_1, x_2, \dots, x_m so that $\mathbf{f}(i) = f(x_i)$. A GP prior for f implies $p(\mathbf{f}|x_1, x_2, \dots, x_m) = \mathcal{N}(0, \Sigma_{\mathbf{ff}})$, where $\Sigma_{\mathbf{ff}} \in \mathbb{R}^{m \times m}$ is the covariance matrix induced from C , with the (i, j) element of $\Sigma_{\mathbf{ff}}$ corresponding to $\text{cov}\{f(x_i), f(x_j)\} = C(x_i, x_j)$, for $1 \leq i, j \leq m$. Prior distribution $\mathcal{N}(0, \Sigma_{\mathbf{ff}})$ can be combined with the information in the likelihood function under model (1) to obtain the posterior distribution, which will be used as a basis for inference.

We want to predict $f(x_i)$, where $x_i \in \mathcal{U}$. Denote $\mathbf{f}_* \in \mathbb{R}^n$ with $\mathbf{f}_*(i) = f(x_{m+i})$ for $i = 1, \dots, n$. Under a GP prior for f , the joint distribution of \mathbf{f} and \mathbf{f}_* is $p(\mathbf{f}, \mathbf{f}_*) = \mathcal{N}(0, \Sigma)$, where Σ is an $(m+n) \times (m+n)$ covariance matrix that can be expressed as $\Sigma = \begin{bmatrix} \Sigma_{\mathbf{ff}} & \Sigma_{\mathbf{ff}_*} \\ \Sigma_{\mathbf{f}_*\mathbf{f}} & \Sigma_{\mathbf{f}_*\mathbf{f}_*} \end{bmatrix}$, where $\Sigma_{\mathbf{ff}_*} \in \mathbb{R}^{m \times n}$, $\Sigma_{\mathbf{f}_*\mathbf{f}} \in \mathbb{R}^{n \times m}$, and $\Sigma_{\mathbf{f}_*\mathbf{f}_*} \in \mathbb{R}^{n \times n}$ are induced from the covariance function C respectively. Denote $\mathbf{y} \in \mathbb{R}^m$ with $\mathbf{y}(i) = y_i$

for $i = 1, \dots, m$ to be the observations over $\{x_1, x_2, \dots, x_m\}$. Under model (1) and a GP prior, we have $p(\mathbf{y}, \mathbf{f}_*) = \mathcal{N}(0, \tilde{\Sigma})$, where

$$\tilde{\Sigma} = \Sigma + \begin{bmatrix} \sigma_{\text{noise}}^2 I_{n \times n} & 0 \\ 0 & 0 \end{bmatrix} = \begin{bmatrix} \Sigma_{\mathbf{f}\mathbf{f}} + \sigma_{\text{noise}}^2 I_{n \times n} & \Sigma_{\mathbf{f}\mathbf{f}_*} \\ \Sigma_{\mathbf{f}_*\mathbf{f}} & \Sigma_{\mathbf{f}_*\mathbf{f}_*} \end{bmatrix}.$$

By a direct calculation, the predictive distribution is

$$p(\mathbf{f}_* | \mathbf{y}) = \mathcal{N}(\Sigma_{\mathbf{f}_*\mathbf{f}}(\Sigma_{\mathbf{f}\mathbf{f}} + \sigma_{\text{noise}}^2 I_{m \times m})^{-1} \mathbf{y}, \Sigma_{\mathbf{f}_*\mathbf{f}_*} - \Sigma_{\mathbf{f}_*\mathbf{f}}(\Sigma_{\mathbf{f}\mathbf{f}} + \sigma_{\text{noise}}^2 I_{m \times m})^{-1} \Sigma_{\mathbf{f}\mathbf{f}_*}).$$

2.2. Graph Laplacian and diffusion based Gaussian process. The graph Laplacian (GL) is a fundamental tool in spectral graph theory [6]. In this section, we first summarize the GL and then introduce the DB-GP, which uses the spectral structure of GL to define a covariance matrix Σ to be used as described in the previous subsection.

Given a dataset $\mathcal{X} = \{x_1, \dots, x_m, x_{m+1}, \dots, x_{m+n}\} \subset \mathbb{R}^D$, we first define a kernel

$$(2) \quad k_\varepsilon(x, x') = \exp\left(-\frac{\|x - x'\|_{\mathbb{R}^D}^2}{4\varepsilon^2}\right),$$

where $\varepsilon > 0$ is a bandwidth parameter. Although we can choose a more general kernel within our proposed methodology, we focus on this Gaussian-like choice for simplicity. This kernel is used to define an $(m+n) \times (m+n)$ affinity matrix W as

$$(3) \quad W_{ij} := \frac{k_\varepsilon(x_i, x_j)}{q_\varepsilon(x_i)q_\varepsilon(x_j)},$$

where $i, j = 1, \dots, m+n$ and $q_\varepsilon(x) := \sum_{i=1}^{m+n} k_\varepsilon(x, x_i)$. We construct an $(m+n) \times (m+n)$ diagonal matrix D so that its i -th diagonal entry is

$$(4) \quad D_{ii} = \sum_{j=1}^{m+n} W_{ij},$$

and define the row stochastic transition matrix as $A = D^{-1}W$. Our main quantity of interest is the GL matrix, which is defined as

$$(5) \quad L := \frac{A - I}{\varepsilon^2}.$$

The affinity matrix W in (3) is symmetric. Hence W can be considered as the affinity matrix of an undirected complete graph $G = (V, E, W)$, where $V = \{x_i\}_{i=1}^{m+n}$ and E consists of edges connecting any pair of points in V , and L is the GL over the affinity graph G . Moreover, the GL can be viewed as an infinitesimal generator of a random walk on G [6]. Note that L is a linear transformation and scaling of A , so on the numerical linear algebra level, we only need to study A . Since A is similar to $\tilde{A} = D^{-1/2}WD^{-1/2}$, \tilde{A} is diagonalizable. The eigenvalues of A and \tilde{A} are the same, with the smallest eigenvalue equal to zero and all the values falling in $[0, 1]$ since the kernel is positive definite.

Proposition 1. *Let μ be an eigenvalue of $-L$. Then $0 \leq \mu \leq \frac{1}{\varepsilon^2}$.*

Remark 1. *The affinity matrix W in (3) is also considered in many kernel based-machine learning algorithms, e.g., diffusion maps [8]. In [8], the term $q_\varepsilon(x)$ is called the α -normalization with $\alpha = 1$. The kernel $k_\varepsilon(x_i, x_j)$ is normalized by q_ε to adjust for the non-uniform sampling density.*

Suppose the dataset $\mathcal{X} = \{x_1, \dots, x_m, x_{m+1}, \dots, x_{m+n}\}$ lies within a subset S of \mathbb{R}^D . We construct the GL matrix L based on \mathcal{X} as in (5). Suppose the eigenpairs of the GL over the affinity graph G are $(-\mu_{i,m+n,\varepsilon}, v_{i,m+n,\varepsilon})$. Denote $\tilde{v}_{i,m+n,\varepsilon}$ to be the eigenvector associated with the eigenvalue $\mu_{i,m+n,\varepsilon}$ of $-L$ normalized in the l^2 norm, where $i = 0, \dots, m+n-1$. By proposition 1, we order $\mu_{i,m+n,\varepsilon}$ so that

$0 = \mu_{0,m+n,\varepsilon} < \mu_{1,m+n,\varepsilon} \leq \dots \leq \mu_{m+n-1,m+n,\varepsilon}$, where $\mu_{0,m+n,\varepsilon} < \mu_{1,m+n,\varepsilon}$ since the graph is connected. Then, we define

$$(6) \quad \mathbf{H}_{\varepsilon,t}^K = (m+n) \sum_{i=0}^{K-1} e^{-\mu_{i,m+n,\varepsilon} t} \tilde{\mathbf{v}}_{i,m+n,\varepsilon} \tilde{\mathbf{v}}_{i,m+n,\varepsilon}^\top \in \mathbb{R}^{(m+n) \times (m+n)},$$

to be the covariance matrix for Gaussian process regression over \mathcal{X} on S . Hence, $\mathbf{H}_{\varepsilon,t}^K$ approximates a diffusion process over G with diffusion time equal to t . For this reason, we refer to a GP with covariance (6) as a DB-GP.

For illustration, we consider a two balloons example in \mathbb{R}^3 . In this case, S is a set with singularities consisting of 2 dimensional spheres and 1 dimensional line segments. We sample 2530 points on S as the dataset \mathcal{X} . Through this toy example, we discuss how the parameters ε , K and t in the DB-GP covariance matrix $\mathbf{H}_{\varepsilon,t}^K$ are related to the geometric structure of set S . We also compare the DB-GP covariance and the normal Gaussian process covariance induced from the squared exponential:

$$(7) \quad \mathbf{C}(x, x') = A \exp\left(-\frac{\|x - x'\|_{\mathbb{R}^D}^2}{\rho^2}\right).$$

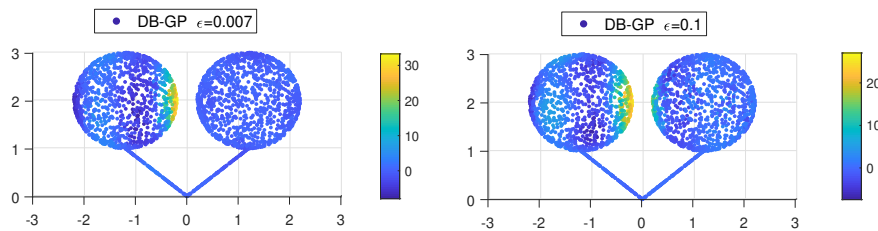


FIGURE 3. When $K = 38$, $t = 0.01$ in $\mathbf{H}_{\varepsilon,t}^K$, we plot a row of DB-GP covariance matrix corresponding to a point in the dataset over the 2530 sampled points on $S \subset \mathbb{R}^3$ for $\varepsilon = 0.007$ and $\varepsilon = 0.1$ respectively.

The parameter ε in the GL should be large enough so that there are sufficient numbers of points in an ε -sized Euclidean neighborhood around x to obtain information about the local geometry but not so large as to include points that are not close to x in intrinsic distance within S . In the two balloons example, we focus on a point x_i located on the right edge of the left balloon; this point is close in Euclidean distance to points on the left edge of the right balloon. We plot the covariance $\mathbf{H}_{\varepsilon,t}^K$ between this point and the other points in Figure 3 letting $K = 38$ and $t = 0.01$. In the left panel, $\varepsilon = 0.007$, which is too small to bridge the gap between the balloons, while in the right panel $\varepsilon = 0.01$, which bridges the gap and leads to inappropriate covariance across balloons. The parameter K controls fluctuations in the DB-GP covariance, with higher frequency oscillations when K is larger. In Figure 4, we plot the covariance relative to the same x as in the previous figure but for different choices of K . When $K = 8$ the covariance decreases monotonically with increasing intrinsic distance from x_i , while for $K = 38$ there are oscillations contributing to non-monotonicity. Finally, the diffusion time t controls the rate of decrease in the covariance as the intrinsic distance increases. Figure 5 shows the impact of varying t on the covariance relative to the impact of varying the bandwidth in the squared exponential covariance.

From the above discussion, we can see that the parameters t , ε and K in the DB-GP covariance have an important impact on performance. We propose to estimate these parameters by maximizing the marginal likelihood,

$$(8) \quad p(\mathbf{y}|\varepsilon, K, t, \sigma_{\text{noise}}) \propto \frac{1}{\det(\mathbf{A} + \sigma_{\text{noise}}^2 \mathbf{I}_{m \times m})} e^{-\mathbf{y}^\top (\mathbf{A} + \sigma_{\text{noise}}^2 \mathbf{I}_{m \times m}) \mathbf{y}};$$

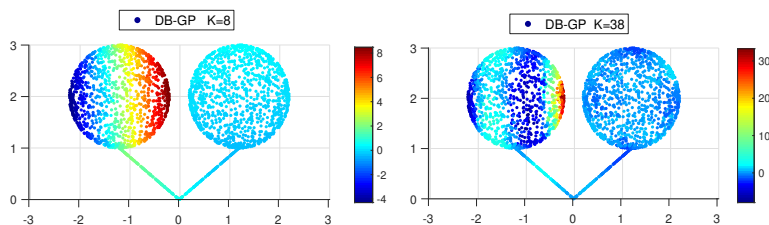


FIGURE 4. When $\varepsilon = 0.007$, $t = 0.01$ in $H_{\varepsilon,t}^K$, we plot a row of DB-GP covariance matrix corresponding to a point in the dataset over the 2530 sampled points on $S \subset \mathbb{R}^3$ for $K = 8$ and $K = 38$ respectively.

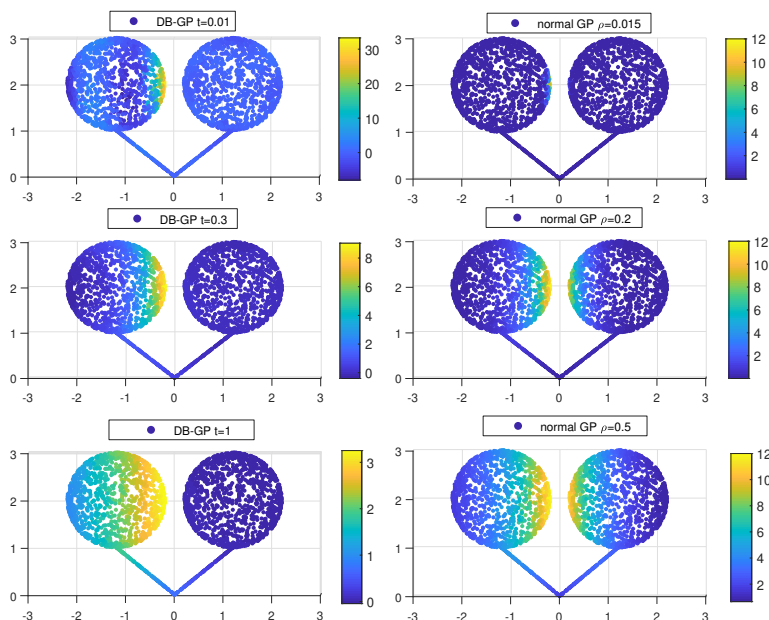


FIGURE 5. When $\varepsilon = 0.007$, $K = 38$ in $H_{\varepsilon,t}^K$, we plot a row of DB-GP covariance matrix corresponding to a point in the dataset over the 2530 sampled points on $S \subset \mathbb{R}^3$ for $t = 0.01$, $t = 0.3$ and $t = 1$ respectively in the three panels on the left. In comparison, we plot the same row of the normal GP covariance matrix over the 2530 sampled points on $S \subset \mathbb{R}^3$ induced by (7) for $A = 12$ and $\rho = 0.015$, $\rho = 0.2$ and $\rho = 0.5$ respectively in the three panels on the right.

an identical strategy to estimate tuning parameters in GP covariance functions is routinely employed in the literature.

The eigen decomposition of the GL leads to a computational complexity of $O((n+m)^3)$ in estimating the DB-GP covariance matrix. Although we do not consider such algorithms further in this paper, there is a vast literature on faster algorithms for obtaining approximate eigen decompositions, and such approaches can potentially be used directly to accelerate the covariance matrix construction step. In addition, in implementing GP computations for a known covariance, we obtain a similar cubic computational complexity in the data size; there is a vast literature on reducing such bottlenecks for GPs and it is of future interest to adapt these algorithms to the DB-GP setting.

3. SIMULATION RESULTS

In this section, we apply our DB-GP approach to simulated datasets. The first case corresponds to the two balloons example, while in the second case data are sampled from a spiral, which is a compact manifold with boundary. For both cases, we compare with the normal GP having covariance (7).

3.1. DB-GP on two balloons. We have two unit spheres centered at $(1.2, 0, 2)$ and $(-1.2, 0, 2)$, respectively. We connect the south poles $(1.2, 0, 1)$ and $(-1.2, 0, 1)$ to the origin by two line segments. Globally, S does not have a manifold structure, and the Hausdorff dimension of S is 2. For simplicity, we sample the labeled points and unlabeled points in the following ways. We sample 30 points randomly based on the uniform probability density function on one of the spheres and sample 3 points randomly based on the uniform probability density function on the attached line segment. Next, we find the 33 points symmetric to the sampled points on the other sphere and line segment. In total, those 66 points are the labeled data points, namely, $\{x_1, \dots, x_{66}\}$. 2200 unlabeled points are sampled in the same way with 2000 points on the spheres and 200 points on the line segment. We enumerate them as $\{x_{67}, \dots, x_{2266}\}$. The labels are sampled under equation (1) with $\sigma_{noise}^2 = 1$ and $f(x) = 5 \times d_S(x, a)$, for $x \in S$, with $a = (-1.2, 0, 3)$ the north pole of the sphere centered at $(-1.2, 0, 2)$ and d_S denoting the distance metric for space S . We plot the labels over x_i for $i = 1, \dots, 66$ and the ground truth in the top two panels in Figure 6.

We use both the DB-GP and the normal GP to predict the response values for the unlabeled data. In both cases, covariance parameters are chosen by maximizing the marginal likelihood and we calculate the root mean square error (RMSE) relative to the true value of the regression function at the unlabeled data points. (8) is maximized when $K = 29$, $\varepsilon = 0.005$, $t = 0.28$ and $\sigma_{noise} = 0.5$, leading to an RMSE of 0.829. Applying the same approach for the normal Gaussian process, we obtain $A = 800$, $\rho = 0.97$, $\sigma_{noise} = 2.9$ and an RMSE of 2.563. Figure 6 compares the prediction by the DB-GP and the normal GP over x_i , for $i = 67, \dots, 2266$. The DB-GP performs better over the regions indicated in the boxes and their symmetric parts on the other sphere. In particular, since the covariance in the normal GP tries to smooth the predictive values between region 1 and its symmetric part, the prediction in region 1 is lower than the true value.

3.2. Spiral case. We consider a spiral M embedded in \mathbb{R}^2 parametrized by

$$\gamma(\theta) = ((\theta + 4)^{0.7} \cos(\theta), (\theta + 4)^{0.7} \sin(\theta)) \in \mathbb{R}^2, \text{ where } \theta \in [0, 8\pi).$$

We randomly sample 60 labeled points $\{\theta_1, \dots, \theta_{60}\}$ and 1500 unlabeled points $\{\theta_{61}, \dots, \theta_{1560}\}$ on $[0, 8\pi)$ based on the uniform probability density function. Let $x_i = \gamma(\theta_i)$ for $i = 1, \dots, 1560$. The labels are sampled under equation (1) with $\sigma_{noise}^2 = 1$ and

$$f(\gamma(\theta)) = 3 \sin\left(\frac{\theta}{10}\right) + 3 \cos\left(\frac{\theta}{2}\right) + 4 \sin\left(\frac{4\theta}{5}\right).$$

We plot the labels over x_i for $i = 1, \dots, 60$, and the ground truth in the top two panels in Figure 7.

Maximizing the marginal likelihoods to choose the covariance parameters, we obtain $K = 9$, $\varepsilon = 0.1$, $t = 0.02$ and $\sigma_{noise} = 1.3$ for the DB-GP, leading to an RMSE of 0.853. For the normal GP, we obtain $A = 17$, $\rho = 2.2$, $\sigma_{noise} = 0.7$ and an RMSE of 1.967. The bottom two panels in Figure 7 show the predictions of the two different approaches. In order to have better visualization, in Figure 8, we plot the predictions over the parameter θ_i of the parametrization. The DB-GP greatly improves predictive performance. As an example, we provide an analysis over region 1. When we ignore the intrinsic geometry of the spiral, based on the response variables over the labeled data, there is a potential increase along the direction outward over region 1. Moreover, for the points that are close to region 1 in Euclidean distance on the inner neighbor arc, the labels are negative and large in magnitude. Hence, the prediction by normal GP over region 1 is negative.

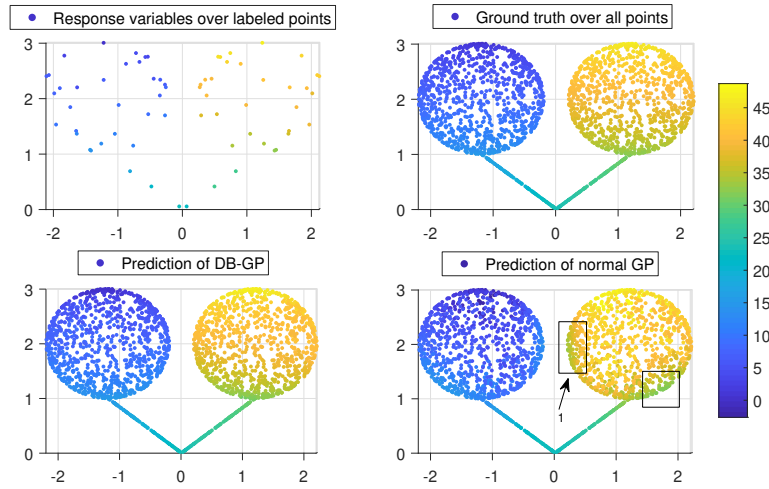


FIGURE 6. The true regression function is 5 times the distance function of a point to the north pole of the sphere on the left. Let $\{x_1, \dots, x_{66}\}$ be the labels points and $\{x_{67}, \dots, x_{2266}\}$ be the unlabeled points. Top left: The plot of the response variables over the labeled points. Top right: The ground truth over all points. Bottom left: The prediction of DB-GP over the unlabeled points with $RMSE = 0.829$. Bottom right: The prediction of normal over the unlabeled points with $RMSE = 2.563$.

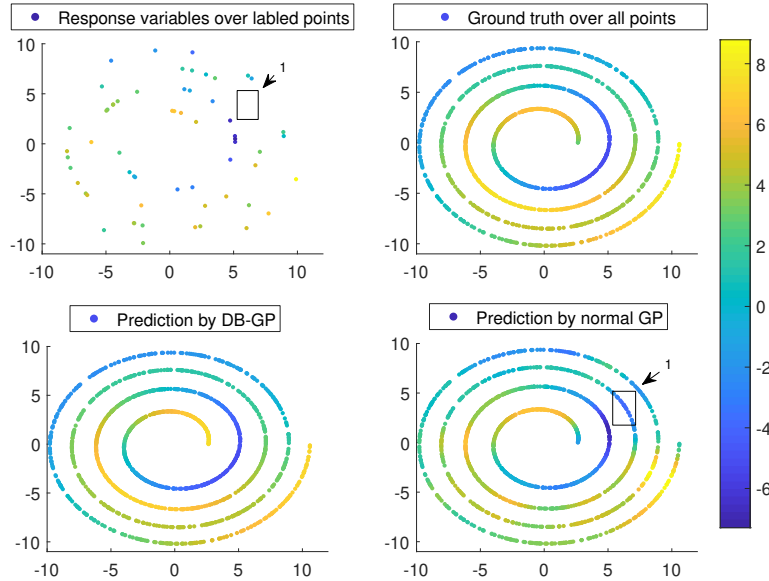


FIGURE 7. Let $\{x_1, \dots, x_{60}\}$ be the labels points and $\{x_{61}, \dots, x_{1560}\}$ be the unlabeled points. Top left: response variables over the labeled points. Top right: ground truth over all points. Bottom left: prediction of DB-GP over the unlabeled points with $RMSE = 0.853$. Bottom right: prediction of the normal GP over the unlabeled points with $RMSE = 1.967$.

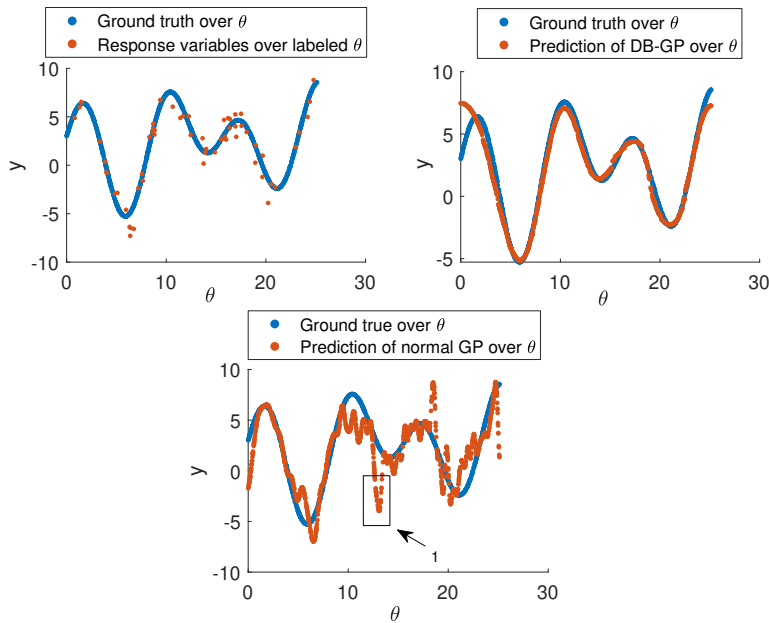


FIGURE 8. Let $\{\theta_1, \dots, \theta_{60}\}$ be the labels parameters and $\{\theta_{61}, \dots, \theta_{1560}\}$ be the unlabeled parameters. Top left: The red points correspond to the response variables over the labeled parameters. The blue points correspond to the ground truth over all $\{\theta_i\}$ for $i = 1, \dots, 1560$. Top Left: The red points represent the prediction of DB-GP over $\{\theta_i\}$ for $i = 61, \dots, 1560$. Bottom: The red points represent the prediction of the normal GP over $\{\theta_i\}$ for $i = 61, \dots, 1560$.

4. APPLICATION TO COASTAL CHLOROPHYLL CONCENTRATION DATA

In this section, we analyze chlorophyll concentration (mg/m^3) along the coasts of the Gulf of California and Long Island. The data reflect the chlorophyll concentration in the corresponding areas in May 2003 and were captured through MODIS (Moderate Resolution Imaging Spectroradiometer) on the Aqua satellite. The data can be found in [1]. We analyze the data using model (1) with a GP prior on the function relating latitude (lat) and longitude (lon) to the expected log chlorophyll concentration, as in the analysis of the Long Island data in Figure 1 presented in Section 1 for the normal GP.

4.1. The coast of Gulf of California. The dataset consists of 1510 points $\{x_1, \dots, x_{1510}\}$ inside the region between longitudes $115^\circ W$ and $110.5^\circ W$ and latitudes $27^\circ N$ and $32^\circ N$. We select a random subset of 73 labeled samples and predict the remaining samples using DB-GP and the normal GP. We evaluate performance based on the RMSE of the predicted values relative to the held out variables. For the DB-GP, we obtained covariance parameters $K = 29$, $\varepsilon = 0.18$, $t = 0.21$ and $\sigma_{noise} = 8$, leading to an RMSE of 3.876. For the normal GP, we obtained $\rho = 0.4$, $A = 150$, $\sigma_{noise} = 15$ and an RMSE of 4.176. Figure 9 shows the predicted values for both approaches. The DB-GP has better performance in boundary regions containing points that are close in Euclidean distance but far away in intrinsic distance; in particular, region 1 in the rectangular box in Figure 9. Focusing on region 2, which has complicated geometry, the RMSE of DB-GP is 4.070 while that of the normal GP is 4.590.

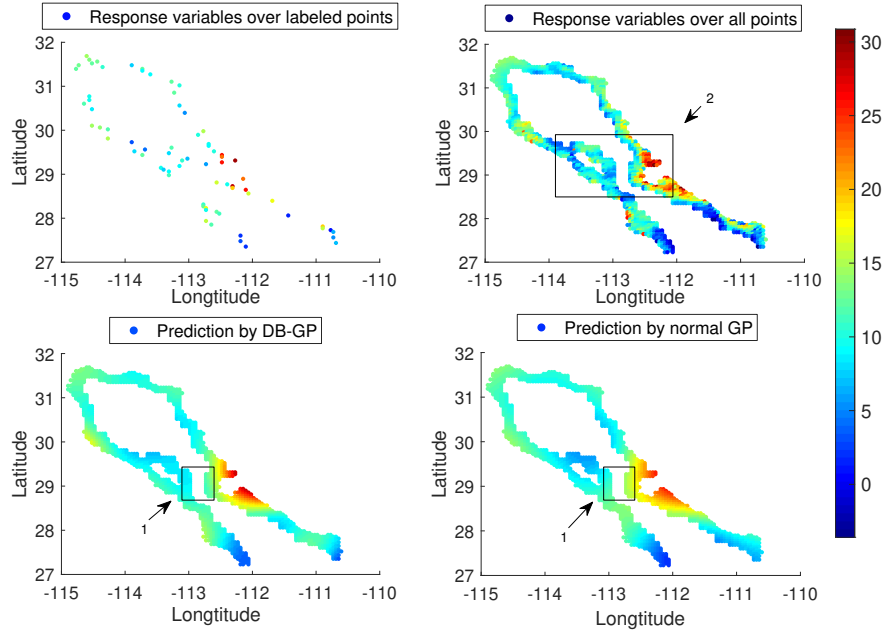


FIGURE 9. The Gulf of California data. Top left: The plot of the response variables over the labeled points $\{x_i\}, i = 1, \dots, 73$. Top right: The plot of the response variables over all points $\{x_i\}, i = 1, \dots, 1510$. Bottom left: the prediction by DB-GP over the unlabeled points $\{x_i\}, i = 74, \dots, 1510$. Bottom right: the prediction by the normal GP over the unlabeled points $\{x_i\}, i = 74, \dots, 1510$.

4.2. The coast of Long Island. In this subsection, we discuss the same dataset as in the illustrative example in the introduction but with different training and test sets. The dataset consists of 914 locations $\{x_1, \dots, x_{914}\}$ in the region between longitudes $71^\circ W$ and $75^\circ W$ and latitudes $39^\circ N$ and $41.5^\circ N$. We randomly select 40 points as labeled samples $\{x_1, \dots, x_{40}\}$ and predict the held-out labels on the remaining 874 samples by the DB-GP and the normal GP respectively.

For the DB-GP, (8) is maximized when $K = 80$, $\varepsilon = 0.007$, $t = 0.03$ and $\sigma_{noise} = 1$, leading to an RMSE of 3.435. Applying the same approach to implement the normal GP, we obtain $\rho = 0.04$, $A = 600$, $\sigma_{noise} = 4$ and an RMSE of 4.967. We plot the predictions over the held-out samples by both approaches in Figure 10.

There are significant differences between the prediction by the normal GP and the observed response variables over regions 1 and 2. This is due to the fact that the labels change relatively smoothly with respect to the intrinsic distance compared with the Euclidean distance. Consider region 1 as an example. The labels indicate a potential decrease in the chlorophyll concentration along $72.6^\circ W$ from $41^\circ N$ to the south in Euclidean distance. As a result, when we apply the normal GP, the prediction around $72.6^\circ W, 40.7^\circ N$ is significantly higher than the true value and the prediction around $72.6^\circ W, 40.5^\circ N$ is significantly lower than the truth. Similar explanations can be applied to region 2.

5. THEORY OF DIFFUSION BASED GAUSSIAN PROCESS

5.1. Diffusion based Gaussian process on subsets of \mathbb{R}^D . In this section, we introduce theory of GLs when the dataset is sampled from a subset S of \mathbb{R}^D . We are going to associate the GL with an integral operator on the set S . Then, we apply spectral theory to the integral operator to define the corresponding

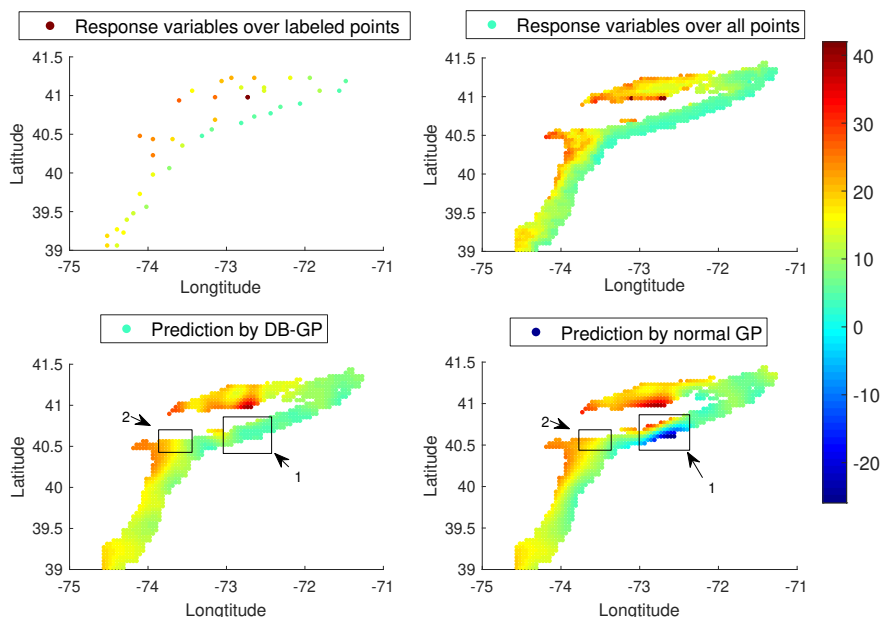


FIGURE 10. Long Island case. Top left: The plot of the response variables over the labeled points $\{x_i\}, i = 1, \dots, 40$. Top right: The plot of the response variables over all points $\{x_i\}, i = 1, \dots, 914$. Bottom left: the prediction by DB-GP over the unlabeled points $\{x_i\}, i = 41, \dots, 914$. Bottom right: the prediction by the normal GP over the unlabeled points $\{x_i\}, i = 41, \dots, 914$.

DB-GP covariance function. We first make the following assumption on the subset S and the probability measure on S .

Assumption 1. Suppose S is a compact connected subset of \mathbb{R}^D . Suppose (S, \mathcal{F}, P) is a probability space, where P is a probability measure defined over the Borel sigma algebra \mathcal{F} on S . Suppose $\mathcal{X} = \{x_1, \dots, x_m, x_{m+1}, \dots, x_{m+n}\}$ are $m+n$ i.i.d. samples based on the measure P .

Remark 2. There are natural measures on S induced by metrics in the ambient Euclidean space \mathbb{R}^D , for example, the d dimensional Hausdorff measure. However, we do not require P to be absolutely continuous with respect to any of these measures.

Based on Assumption 1, we define an integral operator associated with the GL.

Definition 1. For any function $f(x, x')$ on $S \times S$, we define the operator P with respect to the probability measure P as follows,

$$Pf(x) := \int_S f(x, x') dP(x').$$

For the kernel $k_\varepsilon(x, x')$, we define $d_\varepsilon(x) := Pk_\varepsilon(x)$ and $Q_\varepsilon(x, x') := \frac{k_\varepsilon(x, x')}{d_\varepsilon(x)d_\varepsilon(x')}$. For $f(x)$ on S , we define the operator:

$$T_\varepsilon f(x) := \frac{PQ_\varepsilon f(x)}{PQ_\varepsilon(x)} = \frac{\int_S Q_\varepsilon(x, x') f(x') dP(x')}{\int_S Q_\varepsilon(x, x') dP(x')}.$$

The operator T_ε has the following important property. The property motivates our covariance function for the Gaussian process. Hence, we state it as a theorem here. The proof is postponed to Appendix A.

Theorem 1. *Under Assumption 1, for any fixed ε , T_ε is a linear, compact, self-adjoint operator from $L^2(S, \mathbb{P})$ to $L^2(S, \mathbb{P})$. Moreover, suppose A is the matrix in (5) constructed from \mathcal{X} , then for any $f \in L^2(S, \mathbb{P})$, we have the following convergence result: for any $x_k \in \mathcal{X}$,*

$$\lim_{m+n \rightarrow \infty} \sum_{i=1}^{m+n} A_{k,i} f(x_i) = T_\varepsilon f(x_k), \quad a.s.$$

We discuss the theoretical motivation for constructing a covariance function incorporating geometric information about the set S . By Theorem 1, for a fixed ε , since T_ε is compact and self-adjoint, the eigenvalues of $\mathbb{I}_\varepsilon := \frac{\mathbb{I} - T_\varepsilon}{\varepsilon^2}$ satisfy $\lambda_{0,\varepsilon} \leq \lambda_{1,\varepsilon} \leq \dots$. Suppose $(\lambda_{i,\varepsilon}, \phi_{i,\varepsilon})$ is the i -th eigenpair of $\frac{\mathbb{I} - T_\varepsilon}{\varepsilon^2}$ and each $\phi_{i,\varepsilon}$ is normalized in $L^2(S, \mathbb{P})$. Then $\{\phi_{i,\varepsilon}\}$ form an orthonormal basis of $L^2(S, \mathbb{P})$. For any function $f \in L^2(S, \mathbb{P})$, f can be expressed as a unique linear combination of $\{\phi_{i,\varepsilon}\}$, i.e. $f = \sum_{i=0}^{\infty} a_i \phi_{i,\varepsilon}$, a.e. Note that $\sum_{i=1}^{\infty} a_i^2 = \|f\|_{L^2(S, \mathbb{P})}^2 < \infty$. Hence, $a_i \rightarrow 0$ as $i \rightarrow \infty$ and a finite linear combination $\sum_{i=0}^l a_i \phi_{i,\varepsilon}$ is an approximation of f in an $L^2(S, \mathbb{P})$ sense. Based on the above observation, if our unknown regression function is $f \in L^2(S, \mathbb{P})$, it is reasonable to propose a GP covariance function on S by using finitely many eigenpairs of T_ε . More precisely, fixing $K \in \mathbb{N}$ and $t > 0$, we define

$$(9) \quad C_\varepsilon^K(x, x', t) = \sum_{i=0}^{K-1} e^{-\lambda_{i,\varepsilon} t} \phi_{i,\varepsilon}(x) \phi_{i,\varepsilon}(x'),$$

for $x, y \in S$. This covariance function involves three parameters, t , ε and K . The parameter t can be regarded as controlling the bandwidth, and hence the choice of t should depend on the regularity of f . The parameter ε is used in the construction of the operator T_ε over S ; thus, ε should depend on the regularity of S . In contrast, K should depend on both S and the regularity of f .

To formalize this discussion and study the precise relation between S , f and the three parameters, we need to impose a more specific structure on S and more regularity conditions on f . The pointwise convergence of the matrix A to T_ε in Theorem 1 suggests convergence of $H_{\varepsilon,t}^K$ in (6) to $C_\varepsilon^K(x, x', t)$ over the dataset \mathcal{X} as $m+n \rightarrow \infty$. However, to formalize this observation, we need to impose more structure on S . We will discuss this in the next section.

5.2. Diffusion based Gaussian process on manifolds. In this section, we consider the special case in which S has a manifold structure and develop additional theory supporting the DB-GP in this case. Specifically, we make the following assumption.

Assumption 2. *Let M be a d -dimensional smooth, closed and connected Riemannian manifold isometrically embedded in \mathbb{R}^D through $\iota : M \rightarrow \mathbb{R}^D$. Let $S = \iota(M)$. Suppose $(M, \mathcal{F}, \mathbb{P})$ is a probability space, where \mathbb{P} is a probability measure defined over the Borel sigma algebra \mathcal{F} on M . We assume \mathbb{P} is absolutely continuous with respect to the volume measure on M , i.e. $d\mathbb{P} = p dV$ by the Radon-Nikodym theorem, where p is the probability density function on M and dV is the volume form. We further assume p is smooth and is bounded from below by $p_m > 0$. $\mathcal{X} = \{x_1, \dots, x_m, x_{m+1}, \dots, x_{m+n}\}$ are i.i.d. sampled from \mathbb{P} .*

Since ι is an isometry, the function f in model (1) can be equivalently viewed as $f : M \rightarrow \mathbb{R}$ instead of $f : S \rightarrow \mathbb{R}$. We start by modifying the definition of GL and the operator T_ε for datasets and functions on M . Based on Assumption 2, we define the kernel

$$k_\varepsilon(x, x') = \exp\left(-\frac{\|\iota(x) - \iota(x')\|_{\mathbb{R}^D}^2}{4\varepsilon^2}\right),$$

for $x, x' \in M$. We use the kernel $k_\varepsilon(x, x')$ to construct an $(m+n) \times (m+n)$ affinity matrix over \mathcal{X} as in (3). Let L be the graph Laplacian of the affinity graph G with vertices $V = \mathcal{X}$.

In the manifold case, quantities in Definition 1 have the following expansions. For any function $f(x, x')$ on $M \times M$, we have

$$Pf(x) := \int_M f(x, x') dP(x') = \int_M f(x, x') p(x') dV(x').$$

For $f(x)$ on M , we have

$$T_\varepsilon f(x) := \frac{PQ_\varepsilon f(x)}{PQ_\varepsilon(x)} = \frac{\int_S Q_\varepsilon(x, x') f(x') p(x') dV(x')}{\int_S Q_\varepsilon(x, x') p(x') dV(x')}.$$

By the same argument as in Theorem 1, T_ε is a linear, compact, self-adjoint operator from $L^2(M)$ to $L^2(M)$. Since the manifold is compact and smooth, $Q_\varepsilon(x, x')$ is smooth. Hence, $T_\varepsilon f \in C^\infty(M)$. The eigenvalues of $l_\varepsilon = \frac{l - T_\varepsilon}{\varepsilon^2}$ satisfy $\lambda_{0,\varepsilon} \leq \lambda_{1,\varepsilon} \leq \dots$. Suppose $(\lambda_{i,\varepsilon}, \phi_{i,\varepsilon})$ is the i -th eigenpair of $\frac{l - T_\varepsilon}{\varepsilon^2}$ and each $\phi_{i,\varepsilon}$ is normalized in $L^2(M)$. Then $\{\phi_{i,\varepsilon}\}$ form an orthonormal basis of $L^2(M)$.

The covariance function $C_\varepsilon^K(x, x', t)$ under the manifold setup is defined as in (9) for $x, x' \in M$, but is constructed from the GL in a slightly different manner. When S is a general subset of \mathbb{R}^D , we do not impose any other measures on S except the probability measure. However, when M is a Riemannian manifold, there is natural measure, namely the volume measure, induced by the Riemannian metric of the manifold. Hence, the eigenfunctions of l_ε should be normalized in the $L^2(M)$ norm rather than $L^2(M, P)$ norm; proper normalization ensures that the eigenvectors of the GL can approximate the eigenfunctions of l_ε . Hence, we introduce the following definition.

Definition 2. Under Assumption 2, suppose \tilde{v} is an eigenvector of L which is normalized in the l^2 norm. Let $\mathbb{N}(i) = |\mathcal{B}_\varepsilon^{\mathbb{R}^D}(t(x_i)) \cap \{t(x_1), \dots, t(x_{m+n})\}|$, the number of points in an ε ball in \mathbb{R}^D around x_i . Then, we define the l^2 norm of \tilde{v} with respect to the inverse estimated probability density $1/\hat{p}$ as:

$$\|\tilde{v}\|_{l^2(1/\hat{p})} := \sqrt{\frac{|S^{d-1}| \varepsilon^d}{d} \sum_{i=1}^{m+n} \tilde{v}^2(i) \mathbb{N}(i)},$$

where $|S^{d-1}|$ is the volume of the sphere S^{d-1} .

Denote $\mu_{i,m+n,\varepsilon}$ to be the i -th eigenvalue of $-L$ with the associated eigenvector $\tilde{v}_{i,m+n,\varepsilon}$ normalized in the l^2 norm, where $i = 0, \dots, m+n-1$. We order $\mu_{i,m+n,\varepsilon}$ so that $\mu_{0,m+n,\varepsilon} \leq \mu_{1,m+n,\varepsilon} \leq \dots \leq \mu_{m+n-1,m+n,\varepsilon}$. If we define

$$(10) \quad v_{i,m+n,\varepsilon} = \frac{\tilde{v}_{i,m+n,\varepsilon}}{\|\tilde{v}_{i,m+n,\varepsilon}\|_{l^2(1/\hat{p})}},$$

then $v_{i,n,\varepsilon}$ can be regarded as a discretization of some function that is normalized in the $L^2(M)$ norm. Fixing $K \in \mathbb{N}$ and $t > 0$, we define

$$(11) \quad \tilde{H}_{\varepsilon,t}^K = \sum_{i=0}^{K-1} e^{-\mu_{i,m+n,\varepsilon} t} v_{i,m+n,\varepsilon} v_{i,m+n,\varepsilon}^\top \in \mathbb{R}^{(m+n) \times (m+n)}$$

to be the covariance matrix for Gaussian process regression over \mathcal{X} on the manifold M . We summarize the DB-GP algorithm on manifolds in Appendix B.

In Definition 2 we approximate p using a simple 0-1 kernel with bandwidth ε ; refer to [12] for a detailed discussion. When the probability density is uniform, the general DB-GP algorithm in (6) can be viewed as a simplification of (11).

5.3. Convergence of $\tilde{H}_{\varepsilon,t}^K$ to $C_\varepsilon^K(x, x', t)$ under the manifold setup and predictive error. In this section, we show convergence of the covariance matrix $\tilde{H}_{\varepsilon,t}^K$ to the covariance function $C_\varepsilon^K(x, x', t)$ over the dataset $\mathcal{X} = \{x_i\}_{i=1}^{m+n}$ under the manifold setup. More precisely, we provide the convergence rate of entry i, j of the matrix $\tilde{H}_{\varepsilon,t}^K$ to $C_\varepsilon^K(x_i, x_j, t)$ as $m+n \rightarrow \infty$. To state our main theorem, we need to introduce the Laplace Beltrami operator Δ of the manifold M . Here, Δ is an intrinsic differential operator on the

manifold generalizing the notion of the second order derivative on an interval, with the eigenpairs reflecting the geometric and topological structure of the manifold. Let $\sigma(-\Delta) = \{\lambda_i\}_{i=0}^\infty$ be the spectrum of $-\Delta$. By the standard elliptic theory, we have $0 = \lambda_0 < \lambda_1 \leq \lambda_2 \leq \dots$ and each eigenvalue has finite multiplicity. Denote by ϕ_i the eigenfunction normalized in $L^2(M)$ corresponding to λ_i ; that is, for each $i \in \mathbb{N}$, we have $\Delta\phi_i = -\lambda_i\phi_i$. It is well known that $\{\phi_i\}$ forms an orthonormal basis of $L^2(M)$. The main theorem of this section is as follows. The proof of the theorem is in Appendix C.

Theorem 2. *Under Assumption 2, let λ_i be the i -th eigenvalue of $-\Delta$. Fixing $K \in \mathbb{N}$, we let $\Gamma_K := \min_{1 \leq i \leq K} \text{dist}(\lambda_i, \sigma(-\Delta) \setminus \{\lambda_i\})$. If $\varepsilon := \varepsilon(m+n) = (m+n)^{-\frac{1}{4d+15}}$ and $\varepsilon \leq \mathcal{K}_1 \min\left(\left(\frac{\min(\Gamma_K, 1)}{\mathcal{K}_2 + \lambda_K^{d/2+5}}\right)^2, \frac{1}{(2+\lambda_K^{d+1})^2}\right)$, then for any t less than the diameter of M , with probability greater than $1 - (m+n)^{-2}$,*

$$\max_{x_i, x_j \in \mathcal{X}} |\tilde{H}_{\varepsilon, t}^K(i, j) - C_\varepsilon^K(x_i, x_j, t)| \leq \mathcal{K}_3 (\lambda_K^{\frac{d-1}{4}} + 1)^2 K \varepsilon^{1/2},$$

where \mathcal{K}_1 and $\mathcal{K}_2 > 1$ are constants depending on ρ_m , the C^2 norm of \mathfrak{p} , the volume, and the injectivity radius and sectional curvature of the manifold, and \mathcal{K}_3 is a constant depending on ρ_m , the C^2 norm of \mathfrak{p} , the volume, the diameter, the injectivity radius and sectional curvature of the manifold.

Note that $\tilde{H}_{\varepsilon, t}^K$ is composed of the eigenpairs of $-L$, while C_ε^K is composed of the eigenpairs of \mathfrak{l}_ε . Therefore, at first glance, the convergence rate of $\tilde{H}_{\varepsilon, t}^K$ to C_ε^K seems to be irrelevant to the Laplace-Beltrami operator. However, to control the convergence rate, we need to bound the eigengaps, the magnitude of the eigenvalues and the L^∞ norm of the eigenfunctions of \mathfrak{l}_ε , and those terms can be controlled by the eigenvalues of $-\Delta$. The relationship between \mathfrak{l}_ε to $-\Delta$, particularly the spectral convergence when $\varepsilon \rightarrow 0$, is detailed in Proposition 3 in Appendix C. On the other hand, the eigenvalues of $-\Delta$ are completely determined by the geometry of the manifold. Hence, bounding the convergence rate by the eigenvalues of $-\Delta$ shows that the error between $\tilde{H}_{\varepsilon, t}^K$ and C_ε^K is determined by the geometry of the manifold.

Next, we define a $(m+n) \times (m+n)$ matrix Σ so that $\Sigma_{ij} = C_\varepsilon^K(x_i, x_j, t)$. Let $\Sigma = \begin{bmatrix} \Sigma_{11} & \Sigma_{12} \\ \Sigma_{21} & \Sigma_{22} \end{bmatrix}$, where Σ_{11} is a $m \times m$ symmetric matrix. The predictive at $\{x_{m+1}, \dots, x_{m+n}\}$ using the *exact* DB-GP covariance function is then $\mathbf{f}_{\text{DBGP}} := \Sigma_{21}(\Sigma_{11} + \sigma_{\text{noise}}^2 I)^{-1} \mathbf{y}$. The following theorem describes the difference between the predictions of the GP under the matrix $\tilde{H}_{\varepsilon, t}^K$ and the exact DB-GP covariance function. The proof of the theorem is in Appendix D.

Theorem 3. *Fix $\gamma > 0$ and $t > 0$. Suppose $\|\tilde{H}_{\varepsilon, t}^K - \Sigma\|_{\max} \leq \delta(\varepsilon, K) < 1$. Then we have*

$$\|\mathbf{f}_* - \mathbf{f}_{\text{DBGP}}\|_{\max} \leq \frac{m \|\mathbf{y}\|_{\max} ((c + 3\lambda) \|\Sigma_{21}\|_{\max} + \lambda)}{\lambda(\lambda + c\delta(\varepsilon, K))} \delta(\varepsilon, K),$$

where c is a constant depending on $\frac{1}{\delta(\varepsilon, K)}(\tilde{H}_{\varepsilon, t}^K - \Sigma)$ and λ is the smallest eigenvalue of $\Sigma_{11} + \sigma_{\text{noise}}^2 I$.

The DB-GP covariance matrix $\tilde{H}_{\varepsilon, t}^K$ can also be used to recover the heat kernel of the manifold M . The heat kernel on a manifold M is the fundamental solution to the heat equation with an appropriate boundary condition. It describes the diffusion process of the heat flow out of a point on the manifold along the intrinsic distance. Hence, it implies that the covariance structure of DB-GP also varies with respect to the intrinsic distance of the manifold as the bandwidth t in $H_{\varepsilon, t}^K$ changes. We refer the readers to Theorem 3 in [12] for the convergence rate from $H_{\varepsilon, t}^K$ to the heat kernel.

5.4. Measurement error. In this section, we discuss the stability of DB-GP when there are measurement errors, so that the data do not fall exactly on the manifold.

Assumption 3. In addition to Assumption 2, due to measurement error, we assume that the data we observe are $\{x'_1, \dots, x'_n\} \subset \mathbb{R}^D$ such that $\|t(x_i) - x'_i\|_{\mathbb{R}^D} < \delta$, for $i = 1, \dots, n$.

Denote L' to be the GL associated with $\{x'_1, \dots, x'_n\}$. The following theorem shows that if the measurement errors are not too large, then one can still control the eigenvalues and eigenvectors of L' by those of L . The proof of the theorem is in Appendix E.

Theorem 4. Suppose Assumption 3 holds. If $\sqrt{n}\varepsilon^{d+1} \rightarrow \infty$ as $n \rightarrow \infty$ and $\delta < \varepsilon^{d+2}$, there is a constant C such that with probability greater $1 - n^{-2}$, $\|L - L'\|_2 \leq \frac{C}{n^2 \varepsilon^{3d-1}}$, where $\|\cdot\|_2$ is the spectral norm of a matrix.

Remark 3. The error bound on $\|L - L'\|_2$ is of order $\frac{1}{n^2 \varepsilon^{3d-1}}$ because of the $\alpha = 1$ normalization in (3). If the probability density function is uniform, then such normalization is not necessary and the error bound can be improved.

It will be interesting to relax Assumption 3 and allow unbounded measurement error in future work.

5.5. Posterior contraction rate of DB-GP on manifold under the fixed design setup. Let M be a d -dimensional smooth, closed and connected Riemannian manifold with diameter bounded by 1. Assume M is isometrically embedded in \mathbb{R}^D through $\iota : M \rightarrow \mathbb{R}^D$. Let $\lambda_{0,\varepsilon} \leq \lambda_{1,\varepsilon} \leq \dots$ be the eigenvalues of the operator \mathbb{I}_ε . Suppose $\phi_{i,\varepsilon}$ is the i -th eigenfunction of \mathbb{I}_ε and each $\phi_{i,\varepsilon}$ is normalized in $L^2(M)$. We define the following finite dimensional inner product space $\mathbb{H}_{\varepsilon,K,t}$.

Definition 3. For fixed ε, K and $t \geq 0$, we define $\mathbb{H}_{\varepsilon,K,t}$ to be an inner product space on M such that

$$\mathbb{H}_{\varepsilon,K,t} = \left\{ h(x) = \sum_{i=0}^{K-1} a_i e^{-\lambda_{i,\varepsilon} \frac{t}{2}} \phi_{i,\varepsilon}(x), \sum_{i=0}^{K-1} a_i^2 < \infty \right\}$$

with the inner product

$$\left\langle \sum_{i=0}^{K-1} a_i e^{-\lambda_{i,\varepsilon} \frac{t}{2}} \phi_{i,\varepsilon}(x), \sum_{i=0}^{K-1} b_i e^{-\lambda_{i,\varepsilon} \frac{t}{2}} \phi_{i,\varepsilon}(x) \right\rangle_{\mathbb{H}_{\varepsilon,K,t}} := \sum_{i=0}^{K-1} a_i b_i.$$

Denote $E_{\varepsilon,t}^i := e^{-\lambda_{i,\varepsilon} \frac{t}{2}} \phi_{i,\varepsilon}$. Then, $\{E_{\varepsilon,t}^i\}_{i=0}^{K-1}$ is an orthonormal basis of $\mathbb{H}_{\varepsilon,K,t}$. Denote $B_R^{\mathbb{H}_{\varepsilon,K,t}}$ to be the ball of radius R in $\mathbb{H}_{\varepsilon,K,t}$. Also, let $\mathbb{H}_{\varepsilon,K} := \cup_{0 \leq t \leq 1} \mathbb{H}_{\varepsilon,K,t}$.

Refer to Appendix F for basic properties of the spaces $\mathbb{H}_{\varepsilon,K,t}$ and $\mathbb{H}_{\varepsilon,K}$. We explain the reason that we focus our discussion on the space $\mathbb{H}_{\varepsilon,K}$. Any function in $L^\infty(M)$ with certain regularity, for example, a function in the Besov space, can be approximated by the functions in $\cup_\varepsilon \cup_K \mathbb{H}_{\varepsilon,K}$. The Besov space $B_{\infty,\infty}^s$ is a subspace of $L^\infty(M)$ with some regularity quantitatively characterized by the parameter s ; refer to Definition 5 in the Appendix. We state our result as the following approximation proposition. The proposition implies that $\cup_\varepsilon \cup_K \mathbb{H}_{\varepsilon,K}$ is a dense subset of $B_{\infty,\infty}^s$.

Proposition 2. Suppose $\gamma > 0$ is small enough and $f_0 \in B_{\infty,\infty}^s$ with $s > 0$ and $\|f_0\|_\infty \leq 1$. Then there is a function $h \in \mathbb{H}_{\varepsilon,K}$ such that $\|h - f_0\|_\infty \leq \gamma$ and $\|h\|_{\mathbb{H}_{\varepsilon,K,t}}^2 \leq \frac{\text{vol}(M)}{2} \exp[(\gamma/2)^{-2/s} t]$ when $\varepsilon \leq D_1 \gamma^{\frac{2d+s-1}{s}}$ and $K = \lfloor D_2 \gamma^{-\frac{d}{s}} \rfloor$, where D_1 is a constant depending on d, s , the injectivity radius, $\text{vol}(M)$ and the curvature of M and D_2 is a constant depending on d, s and $\text{vol}(M)$.

Through the above Proposition, we construct a stratification indexed by ε and K of a dense subset of $B_{\infty,\infty}^s$. We associate each layer $\mathbb{H}_{\varepsilon,K}$ in the stratification with a Gaussian process. Suppose $\{Z_i\}$ are independent random variables with mean 0 and variance 1. Fix $\varepsilon > 0$ and $K \in \mathbb{N}$. We define a Gaussian process for $t \geq 0$ indexed by $x \in M$,

$$(12) \quad W_{\varepsilon,K}^t(x) := \sum_{i=0}^{K-1} Z_i E_{\varepsilon,t}^i(x) = \sum_{i=0}^{K-1} e^{-\lambda_{i,\varepsilon} \frac{t}{2}} Z_i \phi_{i,\varepsilon}(x).$$

By a straightforward calculation, the covariance function of $W_{\varepsilon,K}^T(x)$, denoted as $C_\varepsilon^K(x, x', t)$, satisfies

$$C_\varepsilon^K(x, x', t) = \mathbb{E}[W_{\varepsilon,K}^T(x)W_{\varepsilon,K}^T(x')] = \sum_{i=0}^{K-1} e^{-\lambda_i \varepsilon t} \phi_{i,\varepsilon}(x)\phi_{i,\varepsilon}(x').$$

Suppose \mathbf{T} is a random variable according to a probability density function g on $[0, 1]$, where g satisfies:

$$(13) \quad \mathcal{C}_1 t^{-p} e^{-t^{-q}} \leq g(t) \leq \mathcal{C}_2 t^{-p} e^{-t^{-q}},$$

for constants $0 < \mathcal{C}_1 \leq \mathcal{C}_2$ and $p, q > 0$. Using g as a prior for $\mathbf{T} = t$ in the DB-GP corresponding to $W_{\varepsilon,K}^T(x)$ leads to a prior Π on $\mathbb{H}_{\varepsilon,K}$.

Assumption 4. *Let M be a d -dimensional smooth, closed and connected Riemannian manifold isometrically embedded in \mathbb{R}^D through $\iota : M \rightarrow \mathbb{R}^D$. We assume that the diameter of M is bounded by 1. We consider the regression model (1) with $\{x_1 \cdots, x_n\} \subset M$. We propose the prior for the regression function f as*

$$W_{\varepsilon,K}^T | \mathbf{T} \sim GP(0, C_\varepsilon^K(x, y, \mathbf{T})) \quad \mathbf{T} \sim g(t),$$

where $g(t)$ is a density function on $[0, 1]$ satisfying (13).

Remark 4. *The assumption that the diameter of M is bounded by 1 is for notation simplicity and the below result holds without this assumption.*

Following [14, 15], given a true function $f_0 \in \mathbb{H}_{\varepsilon,K}$ and a data set $\{(x_1, y_1), \dots, (x_n, y_n)\}$, we say that the *posterior contraction rate* of the Gaussian process prior in the fixed design is at least γ_n if

$$\Pi \left(\frac{1}{n} \sum_{i=1}^n (f(x_i) - f_0(x_i)) \geq \gamma_n \mid \{(x_1, y_1), \dots, (x_n, y_n)\} \right) \rightarrow 0$$

when $n \rightarrow \infty$. We have the following theorem about the posterior contraction rate.

Theorem 5. *Fix any ε and K . Under Assumption 4, suppose $f_0 \in \mathbb{H}_{\varepsilon,K}$ with $\|f_0\|_\infty \leq 1$ and suppose $p \geq 1$, $q \geq \frac{d}{2}$. If we choose $\gamma_n = \left(\frac{n}{\log n}\right)^{-\frac{d}{2q+2d}}$ with $\gamma_n \leq \frac{1}{K}$, then the posterior contraction rate of the Gaussian process prior in the fixed design is at least $2\gamma_n$.*

Remark 5. *For notation simplicity, we assume $\|f_0\|_\infty \leq 1$. A similar result holds with the coefficients in the relation between γ and n depending on $\|f_0\|_\infty$.*

ACKNOWLEDGEMENT

David B Dunson and Nan Wu acknowledge the support from the European Research Council (ERC) under the European Union's Horizon 2020 research and innovation programme (grant agreement No 856506).

REFERENCES

- [1] Dataset title: Chlorophyll-a, Aqua MODIS, NPP, L3SMI, Global, 4km, Science Quality, 2003- present (Monthly Composite). <https://coastwatch.pfeg.noaa.gov/erddap/griddap/erdMH1chlmday.graph>.
- [2] Mikhail Belkin, Partha Niyogi, and Vikas Sindhwani. Manifold regularization: A geometric framework for learning from labeled and unlabeled examples. *Journal of Machine Learning Research*, 7(Nov):2399–2434, 2006.
- [3] Ismaël Castillo, Gérard Kerkycharian, and Dominique Picard. Thomas Bayes' walk on manifolds. *Probability Theory and Related Fields*, 158(3-4):665–710, 2014.
- [4] Françoise Chatelin. *Spectral approximation of linear operators*. Society for Industrial and Applied Mathematics, 2011.
- [5] Ming-Yen Cheng and Hau-Tieng Wu. Local linear regression on manifolds and its geometric interpretation. *Journal of the American Statistical Association*, 108(504):1421–1434, 2013.
- [6] Fan Chung. *Spectral Graph Theory*. American Mathematical Society, 1996.
- [7] Donald L Cohn. *Measure theory*. Springer, 2013.
- [8] Ronald R Coifman and Stéphane Lafon. Diffusion maps. *Applied and Computational Harmonic Analysis*, 21(1):5–30, 2006.

- [9] Richard Courant. Über die Eigenwerte bei den Differentialgleichungen der mathematischen Physik. *Mathematische Zeitschrift*, 7(1):1–57, 1920.
- [10] Harold Donnelly. Eigenfunctions of the Laplacian on compact Riemannian manifolds. *Asian Journal of Mathematics*, 10(1):115–126, 2006.
- [11] Matthew M Dunlop, Dejan Slepčev, Andrew M Stuart, and Matthew Thorpe. Large data and zero noise limits of graph-based semi-supervised learning algorithms. *Applied and Computational Harmonic Analysis*, 2019.
- [12] David B Dunson, Hau-Tieng Wu, and Nan Wu. Spectral convergence of graph Laplacian and Heat kernel reconstruction in L^∞ from random samples. *arXiv preprint arXiv:1912.05680*, 2020.
- [13] Nouredine El Karoui and Hau-Tieng Wu. Graph connection Laplacian methods can be made robust to noise. *The Annals of Statistics*, 44(1):346–372, 2016.
- [14] Subhashis Ghosal, Jayanta K Ghosh, Aad W Van Der Vaart, et al. Convergence rates of posterior distributions. *Annals of Statistics*, 28(2):500–531, 2000.
- [15] Subhashis Ghosal, Aad Van Der Vaart, et al. Convergence rates of posterior distributions for noniid observations. *The Annals of Statistics*, 35(1):192–223, 2007.
- [16] Lars Hörmander. The spectral function of an elliptic operator. *Acta mathematica*, 121(1):193–218, 1968.
- [17] Lizhen Lin, Niu Mu, Pokman Cheung, and David Dunson. Extrinsic Gaussian processes for regression and classification on manifolds. *Bayesian Analysis*, 2018.
- [18] Boaz Nadler, Nathan Srebro, and Xueyuan Zhou. Semi-supervised learning with the graph laplacian: The limit of infinite unlabelled data. *Advances in neural information processing systems*, 22:1330–1338, 2009.
- [19] Mu Niu, Pokman Cheung, Lizhen Lin, Zhenwen Dai, Neil Lawrence, and David Dunson. Intrinsic Gaussian processes on complex constrained domains. *Journal of the Royal Statistical Society: Series B (Statistical Methodology)*, 81(3):603–627, 2019.
- [20] Carl Edward Rasmussen. Gaussian processes in machine learning. In *Summer School on Machine Learning*, pages 63–71. Springer, 2003.
- [21] Aad W van der Vaart and J Harry van Zanten. Rates of contraction of posterior distributions based on Gaussian process priors. *The Annals of Statistics*, 36(3):1435–1463, 2008.
- [22] Aad W van der Vaart, J Harry van Zanten, et al. Reproducing kernel Hilbert spaces of Gaussian priors. In *Pushing the limits of contemporary statistics: contributions in honor of Jayanta K. Ghosh*, pages 200–222. Institute of Mathematical Statistics, 2008.
- [23] Aad W van der Vaart, J Harry van Zanten, et al. Adaptive Bayesian estimation using a Gaussian random field with inverse gamma bandwidth. *The Annals of Statistics*, 37(5B):2655–2675, 2009.
- [24] Xu Wang and Gilad Lerman. Nonparametric Bayesian regression on manifolds via Brownian motion. *arXiv preprint arXiv:1507.06710*, 2015.
- [25] Hau-Tieng Wu and Nan Wu. Think globally, fit locally under the manifold setup: Asymptotic analysis of locally linear embedding. *The Annals of Statistics*, 46(6B):3805–3837, 2018.
- [26] Xiaojin Zhu, Zoubin Ghahramani, and John D Lafferty. Semi-supervised learning using Gaussian fields and harmonic functions. In *Proceedings of the 20th International conference on Machine learning (ICML-03)*, pages 912–919, 2003.
- [27] Xiaojin Jerry Zhu. Semi-supervised learning literature survey. Technical report, University of Wisconsin-Madison Department of Computer Sciences, 2005.

APPENDIX A. PROOF OF THEOREM 1

Clearly T_ε is a linear integral operator. The self-adjointness follows from the fact that $Q_\varepsilon(x, y)$ is symmetric. To show that T_ε is compact, we first show that $\frac{Q_\varepsilon(x, y)}{\int_S Q_\varepsilon(x, y) dP(y)}$ is a Hilbert Schmidt kernel on $S \times S$. Since P is a probability measure, it is σ finite. S is a compact subset of \mathbb{R}^D , the Borel σ algebra \mathcal{F} is countably generated. By Proposition 3.4.5 in [7], $L^2(S, P)$ is a separable Hilbert space. Note that

$$(14) \quad \frac{Q_\varepsilon(x, x')}{\int_S Q_\varepsilon(x, x') dP(x')} = \frac{k_\varepsilon(x, x')}{d_\varepsilon(x') \int_S \frac{k_\varepsilon(x, x')}{d_\varepsilon(x')} dP(x')}$$

Since S is a compact subset of \mathbb{R}^D , the diameter of S in Euclidean distance is bounded above by ℓ . We have $e^{-\frac{\ell^2}{4\varepsilon}} \leq k_\varepsilon(x, x') \leq 1$. Since P is a probability measure, $e^{-\frac{\ell^2}{4\varepsilon}} \leq d_\varepsilon(x) \leq 1$. Substituting the upper and the lower bounds for $k_\varepsilon(x, x')$ and $d_\varepsilon(x)$ into (14), we have $\frac{Q_\varepsilon(x, x')}{\int_S Q_\varepsilon(x, x') dP(x')} \leq e^{\frac{\ell^2}{2\varepsilon}}$. Thus,

$$\int_S \int_S \left| \frac{Q_\varepsilon(x, y)}{\int_S Q_\varepsilon(x, x') dP(x')} \right|^2 dP(x) dP(x') \leq e^{\frac{\ell^2}{\varepsilon}}.$$

Since S is compact and hence locally compact Hausdorff, we conclude that T_ε is a compact operator from $L^2(S, \mathbb{P})$ to $L^2(S, \mathbb{P})$. Finally, we have

$$\begin{aligned} \sum_{i=1}^{m+n} A_{ki} f(x_i) &= \sum_{i=1}^{m+n} \frac{W_{ki} f(x_i)}{D_{kk}} = \frac{\sum_{i=1}^{m+n} W_{ki} f(x_i)}{\sum_{i=1}^{m+n} W_{ki}} \\ &= \frac{\frac{1}{m+n} \sum_{i=1}^{m+n} W_{ki} f(x_i)}{\frac{1}{m+n} \sum_{i=1}^{m+n} W_{ki}} = \frac{\frac{1}{m+n} \sum_{i=1}^{m+n} \frac{k_\varepsilon(x_k, x_i)}{q_\varepsilon(x_k) q_\varepsilon(x_i)} f(x_i)}{\frac{1}{m+n} \sum_{i=1}^{m+n} \frac{k_\varepsilon(x_k, x_i)}{q_\varepsilon(x_k) q_\varepsilon(x_i)}} = \frac{\frac{1}{m+n} \sum_{i=1}^{m+n} \frac{k_\varepsilon(x_k, x_i)}{\frac{1}{m+n} q_\varepsilon(x_k) \frac{1}{m+n} q_\varepsilon(x_i)} f(x_i)}{\frac{1}{m+n} \sum_{i=1}^{m+n} \frac{k_\varepsilon(x_k, x_i)}{\frac{1}{m+n} q_\varepsilon(x_k) \frac{1}{m+n} q_\varepsilon(x_i)}} \\ &= \frac{\frac{1}{m+n} \sum_{i=1}^{m+n} \frac{k_\varepsilon(x_k, x_i)}{\frac{1}{m+n} q_\varepsilon(x_i)} f(x_i)}{\frac{1}{m+n} \sum_{i=1}^{m+n} \frac{k_\varepsilon(x_k, x_i)}{\frac{1}{m+n} q_\varepsilon(x_i)}}. \end{aligned}$$

By the law of large numbers, $\frac{1}{m+n} q_\varepsilon(x_i) \rightarrow d_\varepsilon(x_i)$ as $m+n \rightarrow \infty$ for all x_i a.s. Hence, we have a.s.

$$\frac{\frac{1}{m+n} \sum_{i=1}^{m+n} \frac{k_\varepsilon(x_k, x_i)}{\frac{1}{m+n} q_\varepsilon(x_i)} f(x_i)}{\frac{1}{m+n} \sum_{i=1}^{m+n} \frac{k_\varepsilon(x_k, x_i)}{\frac{1}{m+n} q_\varepsilon(x_i)}} \rightarrow \int_S \frac{k_\varepsilon(x_k, x')}{d_\varepsilon(x')} f(x') d\mathbb{P}(x') = \frac{\int_S Q_\varepsilon(x_k, x') f(x') d\mathbb{P}(x')}{\int_S Q_\varepsilon(x_k, x') d\mathbb{P}(x')} = T_\varepsilon f(x_k).$$

APPENDIX B. ALGORITHM OF DB-GP UNDER THE MANIFOLD SETUP

Algorithm: DB-GP ALGORITHM on manifold

Parameters: Algorithm inputs include ε, t, K and σ_{noise} .

- 1 Construct the $(m+n) \times (m+n)$ matrices W and D as in (3) and (4) by using the kernel

$$k_\varepsilon(x, x') = \exp\left(-\frac{\|\iota(x) - \iota(x')\|_{\mathbb{R}^D}^2}{4\varepsilon^2}\right),$$

and data points $\mathcal{X} = \{x_1, \dots, x_m, x_{m+1}, \dots, x_{m+n}\}$. Let $\tilde{A} = D^{-1/2} W D^{-1/2}$.

- 2 Find the first K eigenpairs of $\frac{\tilde{A}}{\varepsilon^2}$, namely $\{\mu_{i,m+n,\varepsilon}, U_{i,m+n,\varepsilon}\}_{i=0}^{K-1}$. Let $\tilde{v}_{i,m+n,\varepsilon}$ be the normalized vector of $D^{-1/2} U_{i,m+n,\varepsilon}$ in the l^2 norm.
- 3 For $j = 1, \dots, m+n$, find $\mathbb{N}(j) = |\mathcal{B}_\varepsilon^{\mathbb{R}^D}(\iota(x_j)) \cap \{\iota(x_1), \dots, \iota(x_{m+n})\}|$. Calculate

$$\|\tilde{v}_{i,m+n,\varepsilon}\|_{l^2(1/\hat{\rho})} = \sqrt{\frac{|S^{d-1}| \varepsilon^d \sum_{j=1}^{m+n} \tilde{v}_{i,m+n,\varepsilon}^2(j)}{d \mathbb{N}(j)}}.$$

For $i = 0, \dots, K-1$, construct $v_{i,m+n,\varepsilon} = \frac{\tilde{v}_{i,m+n,\varepsilon}}{\|\tilde{v}_{i,m+n,\varepsilon}\|_{l^2(1/\hat{\rho})}}$.

- 4 Construct $\tilde{H}_{\varepsilon,t}^K$ as $\tilde{H}_{\varepsilon,t}^K = \sum_{i=0}^{K-1} e^{-\mu_{i,m+n,\varepsilon} t} v_{i,m+n,\varepsilon} v_{i,m+n,\varepsilon}^\top \in \mathbb{R}^{(m+n) \times (m+n)}$. Rewrite $\tilde{H}_{\varepsilon,t}^K$ as

$$\tilde{H}_{\varepsilon,t}^K = \begin{bmatrix} A & B \\ C & D \end{bmatrix}, \text{ where } A \text{ is an } m \times m \text{ matrix and } B, C, D \text{ are block matrices.}$$

- 5 Let $\mathbf{y} \in \mathbb{R}^m$ be a vector with $\mathbf{y}(i) = y_i$, where y_i is the observed response variable corresponding to x_i . Then $\mathbf{f}_* := C(A + \sigma_{noise}^2 I)^{-1} \mathbf{y}$ is our proposed prediction.
-

APPENDIX C. PROOF OF THEOREM 2

In this section, let $\|\cdot\|_2 := \|\cdot\|_{L^2(M)}$ be the L^2 norm, $\|\cdot\|_\infty := \|\cdot\|_{L^\infty(M)}$ be the L^∞ norm. We have the following fact about the eigenfunctions of the Laplace-Beltrami operator, Δ .

Lemma 1 ([16, 10]). *For a compact Riemannian manifold (M, g) and $l > 0$, we have the following bound for the l -th eigenvalue λ_l and L^2 normalized eigenfunction ϕ_l of the Laplace-Beltrami operator: $\|\phi_l\|_\infty \leq C_1 \lambda_l^{\frac{d-1}{4}} \|\phi_l\|_2 = C_1 \lambda_l^{\frac{d-1}{4}}$, where C_1 is a constant depending on the injectivity radius and sectional curvature of the manifold M .*

The following proposition shows the spectral convergence rate of the first K eigenpairs of the operator $\frac{L-T_\varepsilon}{\varepsilon^2}$ to those of Δ as $\varepsilon \rightarrow 0$.

Proposition 3 ([12] Proposition 1). *Assume that the eigenvalues of Δ are simple. Suppose $(\lambda_{i,\varepsilon}, \phi_{i,\varepsilon})$ is the i -th eigenpair of $\frac{L-T_\varepsilon}{\varepsilon^2}$ and (λ_i, ϕ_i) is the i -th eigenpair of $-\Delta$. Assume both $\phi_{i,\varepsilon}$ and ϕ_i are normalized in the $L^2(M)$ norm. For $K \in \mathbb{N}$, denote $\Gamma_K := \min_{1 \leq i \leq K} \text{dist}(\lambda_i, \sigma(-\Delta) \setminus \{\lambda_i\})$. Suppose $\varepsilon \leq \mathcal{K}_1 \min \left(\left(\frac{\min(\Gamma_K, 1)}{\mathcal{K}_2 + \lambda_K^{\frac{d}{2}+5}} \right)^2, \frac{1}{(2 + \lambda_K^{d+1})^2} \right)$, where \mathcal{K}_1 and $\mathcal{K}_2 > 1$ are constants depending on \mathfrak{p}_m , the C^2 norm of \mathfrak{p} , the volume, and the injectivity radius and sectional curvature of the manifold. Then, there are $a_i \in \{-1, 1\}$ such that for all $i < K$, $|\lambda_{i,\varepsilon} - \lambda_i| \leq \varepsilon^{\frac{3}{2}}$, $\|a_i \phi_{i,\varepsilon} - \phi_i\|_2 \leq \varepsilon^{\frac{3}{2}}$, $\|a_i \phi_{i,\varepsilon} - \phi_i\|_\infty \leq \varepsilon$.*

Remark 6. *We assume that the eigenvalues of Δ are simple to simplify the notation. In the case when the eigenvalues are not simple, the same result still works by introducing the eigenprojection [4].*

In the following proposition, we show that the first K eigenpairs of $-L$ converge to those of $\frac{L-T_\varepsilon}{\varepsilon^2}$ as $m+n \rightarrow \infty$. The proof of the proposition follows from combining Proposition 2, Proposition 3, Proposition 4 in [12], and we omit it.

Proposition 4. *Under Assumption 2, suppose all the eigenvalues of Δ are simple. Let λ_i be the i -th eigenvalue of $-\Delta$. Let $\Gamma_K := \min_{1 \leq i \leq K} \text{dist}(\lambda_i, \sigma(-\Delta) \setminus \{\lambda_i\})$. Let $\mu_{i,m+n,\varepsilon}$ be the i -th eigenvalue of $-L$ with the associated eigenvector $v_{i,m+n,\varepsilon}$ normalized as in (10). Let $(\lambda_{i,\varepsilon}, \phi_{i,\varepsilon})$ be the i -th eigenpair of $\frac{L-T_\varepsilon}{\varepsilon^2}$ with $\phi_{i,\varepsilon}$ normalized in $L^2(M)$. If we choose $\varepsilon = \varepsilon(m+n) = (m+n)^{-\frac{1}{4d+15}}$ and $\varepsilon \leq \mathcal{K}_1 \min \left(\left(\frac{\min(\Gamma_K, 1)}{\mathcal{K}_2 + \lambda_K^{\frac{d}{2}+5}} \right)^2, \frac{1}{(2 + \lambda_K^{d+1})^2} \right)$, then there is a sequence $a_n \in \{1, -1\}$ such that for all $0 \leq i < K$ with probability greater than $1 - (m+n)^{-2}$,*

$$|\mu_{i,n,\varepsilon} - \lambda_{i,\varepsilon}| \leq \Omega_1 \varepsilon^{3/2}, \quad \max_{x_j \in \mathcal{X}} |a_n v_{i,m+n,\varepsilon}(j) - \phi_{i,\varepsilon}(x_j)| \leq \Omega_2 \varepsilon^{1/2},$$

where \mathcal{K}_1 and $\mathcal{K}_2 > 1$ are constants depending on \mathfrak{p}_m , the C^2 norm of \mathfrak{p} , the volume, and the injectivity radius and sectional curvature of the manifold. Ω_1 depends on the curvature of M , \mathfrak{p}_m and the C^1 norm of \mathfrak{p} . Ω_2 depends on the volume and the curvature of M , \mathfrak{p}_m and the C^1 norm of \mathfrak{p} .

With the above proposition, we can prove the uniform convergence of the covariance matrix $\tilde{\mathbb{H}}_{\varepsilon,t}^K$ constructed from the GL to the covariance function $\mathbb{C}_\varepsilon^K(x, x', t)$ over any pair of points (x_i, x_j) . By the triangular inequality, we have

$$\begin{aligned} |\tilde{\mathbb{H}}_{\varepsilon,t}^K(i, j) - \mathbb{C}_\varepsilon^K(x_i, x_j, t)| &= \left| \sum_{l=0}^{K-1} \left(e^{-\mu_{l,m+n,\varepsilon} t} v_{l,m+n,\varepsilon}(i) v_{l,m+n,\varepsilon}^\top(j) - e^{-\lambda_{l,\varepsilon} t} \phi_{l,\varepsilon}(x_i) \phi_{l,\varepsilon}(x_j) \right) \right| \\ &\leq \sum_{l=0}^{K-1} \left(|e^{-\mu_{l,m+n,\varepsilon} t} - e^{-\lambda_{l,\varepsilon} t}| |\phi_{l,\varepsilon}(x_i) \phi_{l,\varepsilon}(x_j)| + |v_{l,m+n,\varepsilon}(i) v_{l,m+n,\varepsilon}^\top(j) - \phi_{l,\varepsilon}(x_i) \phi_{l,\varepsilon}(x_j)| e^{-\mu_{l,m+n,\varepsilon} t} \right). \end{aligned}$$

By Proposition 4, with probability greater than $1 - (m+n)^{-2}$, for all $l < K$,

$$|\mu_{l,m+n,\varepsilon} - \lambda_{l,\varepsilon}| \leq \Omega_1 \varepsilon^{\frac{3}{2}}, \quad \max_{x_i} |a_n v_{l,m+n,\varepsilon}(i) - \phi_{l,\varepsilon}(x_i)| \leq \Omega_2 \varepsilon^{1/2}.$$

By Proposition 1, $\mu_{l,m+n,\varepsilon} \geq 0$. Thus, $|e^{-\mu_{l,m+n,\varepsilon}t}| \leq 1$ and we have

$$\begin{aligned} |e^{-\mu_{l,m+n,\varepsilon}t} - e^{-\lambda_{l,\varepsilon}t}| &\leq |e^{-\mu_{l,m+n,\varepsilon}t}| |1 - e^{(\mu_{l,m+n,\varepsilon} - \lambda_{l,\varepsilon})t}| \leq |1 - e^{(\mu_{l,m+n,\varepsilon} - \lambda_{l,\varepsilon})t}| \\ &\leq |\mu_{l,m+n,\varepsilon} - \lambda_{l,\varepsilon}| t e^{|\mu_{l,m+n,\varepsilon} - \lambda_{l,\varepsilon}|t} \leq \Omega_1 \varepsilon^{\frac{3}{2}} t e^{\Omega_1 \varepsilon^{\frac{3}{2}} t} \leq \Omega_1 \varepsilon^{\frac{3}{2}} t e^{\Omega_1 \mathcal{K}_1^{\frac{3}{2}} t}. \end{aligned}$$

Next, we bound $\|\phi_{l,\varepsilon}\|_\infty$. By Proposition 3, for $l < K$, $\|\phi_{l,\varepsilon}\|_\infty \leq \|\phi_l\|_\infty + \varepsilon$. Hence,

$$\|\phi_{0,\varepsilon}\|_\infty \leq \|\phi_0\|_\infty + \varepsilon \leq \frac{1}{\sqrt{\text{vol}(M)}} + \varepsilon.$$

By Lemma 1, for $1 \leq l < K$, $\|\phi_{l,\varepsilon}\|_\infty \leq \|\phi_l\|_\infty + \varepsilon \leq C_1 \lambda_l^{\frac{d-1}{4}} + \varepsilon$. We combine the above two cases and use the fact that $\varepsilon < \mathcal{K}_1$, for all $l < K$,

$$\|\phi_{l,\varepsilon}\|_\infty \leq C_1 \lambda_l^{\frac{d-1}{4}} + \frac{1}{\sqrt{\text{vol}(M)}} + \varepsilon \leq C_1 \lambda_K^{\frac{d-1}{4}} + \frac{1}{\sqrt{\text{vol}(M)}} + \varepsilon \leq C_2 (\lambda_K^{\frac{d-1}{4}} + 1),$$

where $C_2 = C_1 + \frac{1}{\sqrt{\text{vol}(M)}} + \mathcal{K}_1$ which depends on \mathfrak{p}_m , the C^2 norm of \mathfrak{p} , the volume, and the injectivity

radius and sectional curvature of the manifold. Therefore, $|\phi_l(x_i)\phi_l(x_j)| \leq C_2^2 (\lambda_K^{\frac{d-1}{4}} + 1)^2$ and

$$|e^{-\mu_{l,m+n,\varepsilon}t} - e^{-\lambda_{l,\varepsilon}t}| |\phi_l(x_i)\phi_l(x_j)| \leq \Omega_1 \varepsilon^{\frac{3}{2}} t e^{\Omega_1 \mathcal{K}_1^{\frac{3}{2}} t} C_2^2 (\lambda_K^{\frac{d-1}{4}} + 1)^2.$$

Next, we bound the term $|v_{l,m+n,\varepsilon}(i)v_{l,m+n,\varepsilon}^\top(j) - \phi_{l,\varepsilon}(x_i)\phi_{l,\varepsilon}(x_j)| |e^{-\mu_{l,m+n,\varepsilon}t}|$. Since $\mu_{l,m+n,\varepsilon} \geq 0$,

$$|v_{l,m+n,\varepsilon}(i)v_{l,m+n,\varepsilon}^\top(j) - \phi_{l,\varepsilon}(x_i)\phi_{l,\varepsilon}(x_j)| |e^{-\mu_{l,m+n,\varepsilon}t}| \leq |v_{l,m+n,\varepsilon}(i)v_{l,m+n,\varepsilon}^\top(j) - \phi_{l,\varepsilon}(x_i)\phi_{l,\varepsilon}(x_j)|.$$

Also, for $l < K$, $|v_{l,m+n,\varepsilon}(i)v_{l,m+n,\varepsilon}^\top(j) - \phi_{l,\varepsilon}(x_i)\phi_{l,\varepsilon}(x_j)|$

$$\begin{aligned} &\leq \max_{x_i} |a_n v_{l,m+n,\varepsilon}(i) - \phi_{l,\varepsilon}(x_i)| (\max_{x_i} |\phi_{l,\varepsilon}(x_i)| + \max_{x_i} |v_{l,m+n,\varepsilon}(i)|) \\ &\leq (2 \max_{x_i} |\phi_{l,\varepsilon}| + \Omega_2 \varepsilon^{1/2}) \max_{x_i} |a_n v_{l,m+n,\varepsilon}(i) - \phi_{l,\varepsilon}(x_i)| \leq C_2 (\lambda_K^{\frac{d-1}{4}} + 1) \Omega_2 \varepsilon^{1/2}. \end{aligned}$$

In conclusion, we have $|\tilde{\mathbf{H}}_{\varepsilon,t}^K(i,j) - \mathbf{C}_\varepsilon^K(x_i, x_j, t)|$

$$\begin{aligned} &\leq K \left(\Omega_1 \varepsilon^{\frac{3}{2}} t e^{\Omega_1 \mathcal{K}_1^{\frac{3}{2}} t} C_2^2 (\lambda_K^{\frac{d-1}{4}} + 1)^2 + C_2 (\lambda_K^{\frac{d-1}{4}} + 1) \Omega_2 \varepsilon^{1/2} \right) \\ &\leq K \varepsilon^{1/2} \left(\Omega_1 \varepsilon t e^{\Omega_1 \mathcal{K}_1^{\frac{3}{2}} t} C_2^2 (\lambda_K^{\frac{d-1}{4}} + 1)^2 + C_2 (\lambda_K^{\frac{d-1}{4}} + 1) \Omega_2 \right) \\ &\leq K \varepsilon^{1/2} (\Omega_1 \varepsilon (\text{diam}(M)) e^{\Omega_1 \mathcal{K}_1^{\frac{3}{2}} \text{diam}(M)} C_2^2 + C_2 \Omega_2) (\lambda_K^{\frac{d-1}{4}} + 1)^2 = K \varepsilon^{1/2} \mathcal{K}_3 (\lambda_K^{\frac{d-1}{4}} + 1)^2, \end{aligned}$$

where $\mathcal{K}_3 = \Omega_1 \varepsilon (\text{diam}(M)) e^{\Omega_1 \mathcal{K}_1^{\frac{3}{2}} \text{diam}(M)} C_2^2 + C_2 \Omega_2$ which depends on \mathfrak{p}_m , the C^2 norm of \mathfrak{p} , the volume, the diameter, the injectivity radius and sectional curvature of the manifold.

APPENDIX D. PROOF OF THEOREM 3

Note that $\tilde{\mathbf{H}}_{\varepsilon,t}^K$ and Σ are both symmetric. Hence, by our assumption, there is a symmetric $(m+n) \times (m+n)$ matrix E such that $\tilde{\mathbf{H}}_{\varepsilon,t}^K = \Sigma + \delta E$, where E satisfies $\|E\|_\infty = O(1)$. Let $E = \begin{bmatrix} E_{11} & E_{12} \\ E_{21} & E_{22} \end{bmatrix}$, where E_{11} is a symmetric $m \times m$ matrix. Therefore, we have $\mathbf{A} = \Sigma_{11} + \delta E_{11}$ and $\mathbf{C} = \Sigma_{21} + \delta E_{21}$. Suppose $\mathbf{A} + \sigma_{\text{noise}}^2 \mathbf{I}$ has the eigendecomposition $\mathbf{A} + \sigma_{\text{noise}}^2 \mathbf{I} = \bar{\mathbf{U}} \bar{\mathbf{\Lambda}} \bar{\mathbf{U}}^\top$ and $\Sigma_{11} + \sigma_{\text{noise}}^2 \mathbf{I}$ has the eigendecomposition $\Sigma_{11} + \sigma_{\text{noise}}^2 \mathbf{I} = \mathbf{U} \mathbf{\Lambda} \mathbf{U}^\top$. We can apply perturbation theory for real symmetric matrices (Appendix A and

Lemma E.4 in [25]) such that we have $\bar{\Lambda} = \Lambda + \delta\Lambda'$ and $\bar{U} = U\Theta + \delta U'$, where Λ' is a diagonal matrix of order $O(1)$, U' is of order $O(1)$ and $\Theta \in O(m)$ commutes with Λ and Λ^{-1} . Therefore,

$$\mathbf{f}_{\text{DBGP}} - \mathbf{f}_* = C(\Lambda + \sigma_{\text{noise}}^2 I)^{-1} \mathbf{y} - \Sigma_{21}(\Sigma_{11} + \sigma_{\text{noise}}^2 I)^{-1} \mathbf{y},$$

which can be expanded to

$$\begin{aligned} & (\Sigma_{21} + \delta E_{21})(U\Theta + \delta U')(\Lambda + \delta\Lambda')^{-1}(\Theta^\top U^\top + \delta U'^\top) \mathbf{y} - \Sigma_{21}U\Theta\Lambda^{-1}\Theta^\top U^\top \mathbf{y} \\ &= \Sigma_{21}U\Theta[(\Lambda + \delta\Lambda')^{-1} - \Lambda^{-1}]\Theta^\top U^\top \mathbf{y} + \delta\Sigma_{21}U\Theta(\Lambda + \delta\Lambda')^{-1}U'^\top \mathbf{y} \\ & \quad + \delta\Sigma_{21}U'(\Lambda + \delta\Lambda')^{-1}\Theta^\top U'^\top \mathbf{y} + \delta^2\Sigma_{21}U'(\Lambda + \delta\Lambda')^{-1}U'^\top \mathbf{y} \\ & \quad + \delta E_{21}(U\Theta + \delta U')(\Lambda + \delta\Lambda')^{-1}(\Theta^\top U^\top + \delta U'^\top) \mathbf{y}. \end{aligned}$$

Note that $\|(\Lambda + \delta\Lambda')^{-1}\|_{\max} \leq \frac{1}{\lambda + c\delta}$ and $\|(\Lambda + \delta\Lambda')^{-1} - \Lambda^{-1}\|_{\max} \leq \frac{c\delta}{\lambda(\lambda + c\delta)}$, where c is a constant depending on E_{11} . Therefore, we have that

$$\begin{aligned} \|\mathbf{f}_{\text{DBGP}} - \mathbf{f}_*\|_{\max} &\leq \frac{c\delta\|\Sigma_{21}\mathbf{y}\|_{\max}}{\lambda(\lambda + c\delta)} + \frac{2\delta\|\Sigma_{21}\mathbf{y}\|_{\max}}{\lambda + c\delta} + \frac{\delta^2\|\Sigma_{21}\mathbf{y}\|_{\max}}{\lambda + c\delta} + \frac{m\delta\|\mathbf{y}\|_{\max}}{\lambda + c\delta} \\ &\leq \frac{\delta m\|\mathbf{y}\|_{\max}((c + 3\lambda)\|\Sigma_{21}\|_{\max} + \lambda)}{\lambda(\lambda + c\delta)}. \end{aligned}$$

APPENDIX E. PROOF OF THEOREM 4

For any pairs x_i, x_j and x'_i, x'_j , without loss of generality, we assume $\|\mathbf{u}(x_i) - \mathbf{u}(x_j)\|_{\mathbb{R}^D} < \|x'_i - x'_j\|_{\mathbb{R}^D}$. Then, a sequence of trivial bounds leads to

$$\begin{aligned} & |k_\varepsilon(x_i, x_j) - k_\varepsilon(x'_i, x'_j)| \\ &= \left| \exp\left(-\frac{\|\mathbf{u}(x_i) - \mathbf{u}(x_j)\|_{\mathbb{R}^D}^2}{4\varepsilon^2}\right) - \exp\left(-\frac{\|x'_i - x'_j\|_{\mathbb{R}^D}^2}{4\varepsilon^2}\right) \right| \\ &\leq \exp\left(-\frac{\|\mathbf{u}(x_i) - \mathbf{u}(x_j)\|_{\mathbb{R}^D}^2}{4\varepsilon^2}\right) \left| \frac{\|\mathbf{u}(x_i) - \mathbf{u}(x_j)\|_{\mathbb{R}^D}^2 - \|x'_i - x'_j\|_{\mathbb{R}^D}^2}{4\varepsilon^2} \right| \\ &\leq \exp\left(-\frac{\|\mathbf{u}(x_i) - \mathbf{u}(x_j)\|_{\mathbb{R}^D}^2}{4\varepsilon^2}\right) \left| \|\mathbf{u}(x_i) - \mathbf{u}(x_j)\|_{\mathbb{R}^D} - \|x'_i - x'_j\|_{\mathbb{R}^D} \right| \frac{\|\mathbf{u}(x_i) - \mathbf{u}(x_j)\|_{\mathbb{R}^D} + \|x'_i - x'_j\|_{\mathbb{R}^D}}{4\varepsilon^2} \\ &\leq \frac{2\delta}{\varepsilon} \exp\left(-\frac{\|\mathbf{u}(x_i) - \mathbf{u}(x_j)\|_{\mathbb{R}^D}^2}{4\varepsilon^2}\right) \left(\frac{\|\mathbf{u}(x_i) - \mathbf{u}(x_j)\|_{\mathbb{R}^D}}{2\varepsilon} + \frac{\delta}{4\varepsilon} \right) \leq \frac{2\delta}{\varepsilon} \left(\frac{1}{2} + \frac{\delta}{4\varepsilon} \right) \leq \frac{2\delta}{\varepsilon}. \end{aligned}$$

Note that we use the fact that $a \exp(-a^2) < \frac{1}{2}$ for any $a > 0$ in the second to last step. Hence, for any i , $|q_\varepsilon(x_i) - q_\varepsilon(x'_i)| < \frac{2n\delta}{\varepsilon}$. Similarly, we can show that

$$\exp\left(-\frac{2\text{diam}(M)\delta}{\varepsilon^2}\right) \leq \frac{k_\varepsilon(x_i, x_j)}{k_\varepsilon(x'_i, x'_j)} \leq \exp\left(\frac{2\text{diam}(M)\delta}{\varepsilon^2}\right),$$

where $\text{diam}(M)$ is the diameter of the manifold. Thus, for any i ,

$$\exp\left(-\frac{2\text{diam}(M)\delta}{2\varepsilon^2}\right) q_\varepsilon(x_i) < q_\varepsilon(x'_i), \quad k_\varepsilon(x'_i, x'_j) \leq \exp\left(\frac{2\text{diam}(M)\delta}{\varepsilon^2}\right).$$

By Lemma 10 in [12], if $\sqrt{n}\varepsilon^{d+1} \rightarrow \infty$ as $n \rightarrow \infty$, then with probability greater $1 - n^{-2}$, $C_1 n \varepsilon^d < q_\varepsilon(x_i) < C_2 n \varepsilon^d$. So, $C_1 \exp\left(-\frac{2\text{diam}(M)\delta}{\varepsilon^2}\right) n \varepsilon^d < q_\varepsilon(x'_i)$, and hence

$$\begin{aligned} |W_{ij} - W'_{ij}| &\leq \frac{|k_\varepsilon(x_i, x_j) - k_\varepsilon(x'_i, x'_j)|}{q_\varepsilon(x_i)q_\varepsilon(x_j)} + k_\varepsilon(x'_i, x'_j) \left(\frac{|q_\varepsilon(x_i) - q_\varepsilon(x'_i)|}{q_\varepsilon(x_i)q_\varepsilon(x'_i)q_\varepsilon(x'_j)} + \frac{|q_\varepsilon(x_j) - q_\varepsilon(x'_j)|}{q_\varepsilon(x_i)q_\varepsilon(x_j)q_\varepsilon(x'_j)} \right) \\ &\leq \frac{2\delta}{C_1^2 n^2 \varepsilon^{2d+1}} + \frac{2 \exp\left(\frac{6\text{diam}(M)\delta}{\varepsilon^2}\right) \delta}{C_1^2 n^3 \varepsilon^{3d+1}} < \frac{5}{C_1^2 n^2 \varepsilon^{d-1}}, \end{aligned}$$

where we use the fact that $\delta < \varepsilon^{d+2}$ and $n\varepsilon^d \rightarrow \infty$ in the last step. Also, $\gamma_1 := \max_{i,j} W_{ij} \leq \frac{1}{C_1^2 n^2 \varepsilon^{2d}}$ and

$$\begin{aligned} \gamma_2 &:= \min_i \sum_{j \neq i} \frac{W_{ij}}{n} = \min_i \sum_{j \neq i} \frac{k_\varepsilon(x_i, x_j)}{n q_\varepsilon(x_i) q_\varepsilon(x_j)} > \frac{1}{C_2^2 n^3 \varepsilon^{2d}} \min_i \sum_{j \neq i} k_\varepsilon(x_i, x_j) \\ &= \frac{1}{C_2^2 n^3 \varepsilon^{2d}} \min_i (q_\varepsilon(x_i) - 1) > \frac{C_1 n \varepsilon^d - 1}{C_2^2 n^3 \varepsilon^{2d}} = \frac{C_1 - \frac{1}{n \varepsilon^d}}{C_2^2 n^2 \varepsilon^d}. \end{aligned}$$

Therefore, by Lemma 2.1 in [13],

$$\|L - L'\|_2 \leq \frac{1}{\gamma_2} \frac{5}{C_1^2 n^2 \varepsilon^{d-1}} + \frac{\gamma_1^2}{\gamma_2 \left(\gamma_2 - \frac{4}{C_1^2 n^2 \varepsilon^{d-1}} \right)} \frac{5}{C_1^2 n^2 \varepsilon^{d-1}} \leq \frac{C}{n^2 \varepsilon^{3d-1}}.$$

APPENDIX F. PROOFS OF THEOREM 5

We discuss some properties of the inner product space $\mathbb{H}_{\varepsilon, K, t}$. First, we have the following bounds controlling $\|\cdot\|_{\mathbb{H}_{\varepsilon, K, t}}$. The proof follows directly from the fact that M is compact and $\{\phi_{i, \varepsilon}\}$ forms an orthonormal basis of $L^2(M)$ and we omit details.

Proposition 5. Fix $\varepsilon > 0$, $K \in \mathbb{N}$ and $t \geq 0$. For $f \in \mathbb{H}_{\varepsilon, K, t}$, $e^{-\lambda_{K-1, \varepsilon} t} \|f\|_{\mathbb{H}_{\varepsilon, K, t}}^2 \leq \|f\|_2 \leq \text{vol}(M) \|f\|_\infty^2$.

Hence, for any $\varepsilon > 0$, $K \in \mathbb{N}$ and $0 \leq t \leq 1$, we have $\mathbb{H}_{\varepsilon, K, t} \subset \mathbb{H}_{\varepsilon, K} \subset L^\infty(M)$. Also, note that for fixed ε and K , the spaces $\mathbb{H}_{\varepsilon, K, t}$ are isomorphic for all $t \geq 0$. Moreover, we have the following nested sequence of unit balls.

Proposition 6. Fix $\varepsilon > 0$ and $K \in \mathbb{N}$. If $0 \leq t_1 \leq t_2$, then $B_1^{\mathbb{H}_{\varepsilon, K, t_2}} \subset B_1^{\mathbb{H}_{\varepsilon, K, t_1}}$.

Proof. $f(x) = \sum_{i=0}^{K-1} b_i e^{-\lambda_{i, \varepsilon} \frac{t_2}{2}} \phi_{i, \varepsilon}(x) \in B_1^{\mathbb{H}_{\varepsilon, K, t_2}}$ can be written as $f(x) = \sum_{i=0}^{K-1} a_i e^{-\lambda_{i, \varepsilon} \frac{t_1}{2}} \phi_{i, \varepsilon}(x)$ for $t_1 \leq t_2$. Then we have $a_i e^{-\lambda_{i, \varepsilon} \frac{t_1}{2}} = b_i e^{-\lambda_{i, \varepsilon} \frac{t_2}{2}}$. Since $t_1 \leq t_2$, we have $a_i \leq b_i$. Hence, $\sum_{i=0}^{K-1} a_i^2 \leq \sum_{i=0}^{K-1} b_i^2 \leq 1$. In other words, we have $f(x) \in B_1^{\mathbb{H}_{\varepsilon, K, t_1}}$. Hence, $B_1^{\mathbb{H}_{\varepsilon, K, t_2}} \subset B_1^{\mathbb{H}_{\varepsilon, K, t_1}}$. \square

We need the following fact about the eigenfunctions of the Laplace-Beltrami operator, Δ .

Lemma 2 (Weyl's law [9]). For a compact and connected Riemannian manifold (M, g) , the eigenvalues of the Laplace-Beltrami operator $0 = \lambda_0 < \lambda_1 \leq \dots$ satisfy $l = C_2 \lambda_l^{d/2} + O(\lambda_l^{\frac{d-1}{2}} \log \lambda_l)$, where C_2 is a constant depending on the volume of the manifold. For K large enough, we have $\lambda_{K-1} \leq C_3 K^{\frac{2}{d}}$, where $C_3 = \left(\frac{2}{C_2}\right)^{\frac{2}{d}}$.

Next, we recall some definitions about Littlewood-Paley theory in smooth functional calculus. We first construct a bump function Ψ , or father wavelet, satisfying the following conditions: (1) $\Psi \in C^\infty(\mathbb{R}_{\geq 0})$ with support in $[0, 1]$, (2) $0 \leq \Psi(x) \leq 1$ when $x \geq 0.5$, (3) $\Psi(x) = 1$ for $0 \leq x \leq 0.5$, (4) $\Psi'(x) \leq \mathcal{C}$ for some $\mathcal{C} > 0$.

Definition 4. Fix $\delta > 0$ and $\varepsilon > 0$. We define the following integral kernels and operators:

$$\Psi(\delta\sqrt{\Delta})(x, x') := \sum_{i=0}^{\infty} \Psi(\delta\sqrt{\lambda_i})\phi_i(x)\phi_i(x'), \quad \Psi_K(\delta\sqrt{I_\varepsilon})(x, x') := \sum_{i=0}^{K-1} \Psi(\delta\sqrt{\lambda_{i,\varepsilon}})\phi_{i,\varepsilon}(x)\phi_{i,\varepsilon}(x').$$

The corresponding integral operators are defined as

$$\Psi(\delta\sqrt{\Delta})f(x) = \int_M \Psi(\delta\sqrt{\Delta})(x, x')f(x')dV(x'), \quad \Psi_K(\delta\sqrt{I_\varepsilon})f(x) = \int_M \Psi_K(\delta\sqrt{I_\varepsilon})(x, x')f(x')dV(x').$$

Set $\Psi_j(x) = \Psi(2^{-j}x)$ for $j \geq 0$. We can thus define the Besov space we are interested in this paper.

Definition 5. (Besov space) Fix $s > 0$. $f \in B_{\infty,\infty}^s$ if $f \in L^\infty(M)$ and

$$\|f\|_{B_{\infty,\infty}^s} := \sup_j 2^{sj} \|\Psi_j(\sqrt{\Delta})f - f\|_\infty < \infty.$$

The above definition is independent of the choice of bump function Ψ .

Proof of Proposition 2

Proof. If $f_0 \in B_{\infty,\infty}^s$, then by definition we have $\|\Psi(\delta\sqrt{\Delta})f_0 - f_0\|_\infty \leq C\delta^s$ for some $C > 0$. Denote $\gamma := 2C\delta^s$. For a small δ , by the definition of Ψ , we have

$$(15) \quad \|\Psi(\delta\sqrt{\Delta})f_0 - f_0\|_\infty = \left\| \int_M \sum_{\lambda_i \leq \delta^{-2}} \Psi(\delta\sqrt{\lambda_i})\phi_i(x)\phi_i(x')f_0(x')dV(x') - f_0 \right\|_\infty \leq C\delta^s = \gamma/2.$$

By Weyl's law, we have $\lambda_{K-1} \leq C_3K^{\frac{2}{d}}$, where $C_3 = (\frac{2}{C_2})^{\frac{2}{d}}$. Suppose K satisfies $C_3K^{\frac{2}{d}} \leq \delta^{-2} = (\frac{\gamma}{2C})^{\frac{2}{s}}$, i.e. $K \leq C_3^{-\frac{d}{2}}(2C)^{\frac{d}{s}}\gamma^{-\frac{d}{s}}$, which leads to $\lambda_{K-1} \leq \delta^{-2}$. Therefore, if we choose $K = \lfloor C_3^{-\frac{d}{2}}(2C)^{\frac{d}{s}}\gamma^{-\frac{d}{s}} \rfloor = \lfloor D_2\gamma^{-\frac{d}{s}} \rfloor$, we have $\Psi(\delta\sqrt{\Delta})f_0 = \int_M \sum_{i=0}^{K-1} \Psi(\delta\sqrt{\lambda_i})\phi_i(x)\phi_i(x')f_0(x')dV(x')$.

Next, we find a suitable ε so that $\int_M \sum_{i=0}^{K-1} \Psi(\delta\sqrt{\lambda_i})\phi_i(x)\phi_i(x')f_0(x')dV(x')$ can be well controlled by $\Psi_K(\delta\sqrt{I_\varepsilon})f_0(x)$. It comes from a sequence of bounds.

$$\begin{aligned} & \left\| \Psi_K(\delta\sqrt{I_\varepsilon})f_0(x) - \int_M \sum_{i=0}^{K-1} \Psi(\delta\sqrt{\lambda_i})\phi_i(x)\phi_i(x')f_0(x')dV(x') \right\|_\infty \\ & \leq C_4(K-1) \max_{1 \leq i \leq K-1} \left\| \left[\Psi(\delta\sqrt{\lambda_{i,\varepsilon}}) - \Psi(\delta\sqrt{\lambda_i}) \right] \phi_i(x)\phi_i(x') + \Psi(\delta\sqrt{\lambda_{i,\varepsilon}}) [\phi_{i,\varepsilon}(x)\phi_{i,\varepsilon}(x') - \phi_i(x)\phi_i(x')] \right\|_\infty \\ & \leq C_4(K-1) \left(\max_{1 \leq i \leq K-1} \left| \Psi(\delta\sqrt{\lambda_{i,\varepsilon}}) - \Psi(\delta\sqrt{\lambda_i}) \right| \max_{1 \leq i \leq K-1} \|\phi_i\|_\infty^2 + \max_{1 \leq i \leq K-1} \|\phi_{i,\varepsilon}(x)\phi_{i,\varepsilon}(x') - \phi_i(x)\phi_i(x')\|_\infty \right), \end{aligned}$$

where we bound $\Psi(\delta\sqrt{\lambda_{i,\varepsilon}})$ by 1. Applying Proposition 3, the right hand side is further bounded by

$$\begin{aligned} & C_4(K-1) \left(\max_{1 \leq i \leq K-1} \mathcal{C}\delta \left| \sqrt{\lambda_{i,\varepsilon}} - \sqrt{\lambda_i} \right| C_1^2 \lambda_{K-1}^{\frac{d-1}{2}} + \max_{1 \leq i \leq K-1} \|\phi_{i,\varepsilon} - \phi_i\|_\infty (\|\phi_{i,\varepsilon}\|_\infty + \|\phi_i\|_\infty) \right) \\ & \leq C_4K \left(\mathcal{C}C_1^2\delta \max_{1 \leq i \leq K-1} \frac{|\lambda_{i,\varepsilon} - \lambda_i|}{\sqrt{\lambda_{i,\varepsilon}} + \sqrt{\lambda_i}} \lambda_{K-1}^{\frac{d-1}{2}} + \max_{1 \leq i \leq K-1} \|\phi_{i,\varepsilon} - \phi_i\|_\infty (\|\phi_{i,\varepsilon}\|_\infty + \|\phi_i\|_\infty) \right) \\ (16) \quad & \leq C_4K \left(\mathcal{C}C_1^2\delta^{2-d} \frac{\varepsilon^{\frac{3}{2}}}{\sqrt{\lambda_1}} + \max_{1 \leq i \leq K-1} \varepsilon(2\|\phi_i\|_\infty + \varepsilon) \right). \end{aligned}$$

To finish the proof, (16) is further controlled by

$$\begin{aligned}
& C_4 K \left(\mathcal{C} C_1^2 \delta^{2-d} \frac{\varepsilon^{\frac{3}{2}}}{\sqrt{\lambda_1}} + \varepsilon (2C_1 \lambda_{K-1}^{\frac{d-1}{4}} + \varepsilon) \right) \\
& \leq C_4 C_3^{\frac{d}{2}} \delta^{-d} \left(\mathcal{C} C_1^2 \delta^{2-d} \frac{\varepsilon^{\frac{3}{2}}}{\sqrt{\lambda_1}} + \varepsilon (2C_1 \delta^{\frac{1-d}{2}} + \varepsilon) \right) \\
& \leq C_4 C_3^{\frac{d}{2}} \delta^{-d} \left(\mathcal{C} C_1^2 \delta^{2-d} \frac{\varepsilon^{\frac{3}{2}}}{\sqrt{\lambda_1}} + \varepsilon (3C_1 \delta^{\frac{1-d}{2}}) \right) \\
& \leq C_4 C_3^{\frac{d}{2}} \left(\frac{\mathcal{C} C_1^2}{\sqrt{\lambda_1}} + 3C_1 \right) \varepsilon \delta^{1-2d} = C_4 C_3^{\frac{d}{2}} \left(\frac{\mathcal{C} C_1^2}{\sqrt{\lambda_1}} + 3C_1 \right) \varepsilon \left(\frac{\gamma}{2C} \right)^{\frac{1-2d}{s}},
\end{aligned}$$

where we use the fact that both δ^{2-2d} and $\delta^{\frac{1-3d}{2}}$ are bounded by δ^{1-2d} for $d \geq 1$ in the second last step. Clearly, if we have

$$\varepsilon \leq \frac{1}{2} (2C)^{\frac{1-2d}{s}} \left[C_4 C_3^{\frac{d}{2}} \left(\frac{\mathcal{C} C_1^2}{\sqrt{\lambda_1}} + 3C_1 \right) \right]^{-1} \gamma^{\frac{2d+s-1}{s}},$$

then we have

$$\begin{aligned}
(17) \quad & \left\| \Psi_K(\delta\sqrt{\varepsilon})f_0(x) - \int_M \sum_{i=0}^{K-1} \Psi(\delta\sqrt{\lambda_i})\phi_i(x)\phi_i(x')f_0(x')dV(x') \right\|_{\infty} \\
& \leq C_4 C_3^{\frac{d}{2}} \left(\frac{\mathcal{C} C_1^2}{\sqrt{\lambda_1}} + 3C_1 \right) \varepsilon \left(\frac{\gamma}{2C} \right)^{\frac{1-2d}{s}} \leq \frac{\gamma}{2}.
\end{aligned}$$

Denote $D_1 := \frac{1}{2} (2C)^{\frac{1-2d}{s}} \left[C_4 C_3^{\frac{d}{2}} \left(\frac{\mathcal{C} C_1^2}{\sqrt{\lambda_1}} + 3C_1 \right) \right]^{-1}$. By (15) and (17), we have $\|\Psi_K(\delta\sqrt{\varepsilon})f_0 - f_0\|_{\infty} \leq \gamma$. Let $h(x) := \Psi_K(\delta\sqrt{\varepsilon})f_0(x)$. To finish the proof, we claim that $h \in \mathbb{H}_{\varepsilon, K}$. Since $\{\phi_{i, \varepsilon}\}$ form a basis of $L^2(M)$, we have $\|f_0\|_2^2 = \sum_{i=0}^{\infty} \left| \int_M \phi_{i, \varepsilon}(y)f_0(y)dV(y) \right|^2$. Therefore, by the assumption of f_0 , we have

$$\sum_{i=0}^{K-1} \left| \int_M \phi_{i, \varepsilon}(y)f_0(y)dV(y) \right|^2 \leq \|f_0\|_2^2 \leq \text{vol}(M).$$

As a result, by a direct bound, we have

$$\begin{aligned}
\|h\|_{\mathbb{H}_{\varepsilon, K, t}}^2 &= \left\| \int_M \sum_{i=0}^{K-1} \Psi(\delta\sqrt{\lambda_{i, \varepsilon}})\phi_{i, \varepsilon}(x)\phi_{i, \varepsilon}(x')f_0(x')dV(x') \right\|_{\mathbb{H}_{\varepsilon, K, t}}^2 \\
&\leq \left\| \sum_{i=0}^{K-1} \Psi(\delta\sqrt{\lambda_{i, \varepsilon}}) \int_M \phi_{i, \varepsilon}(x')f_0(x')dV(x')\phi_{i, \varepsilon}(x) \right\|_{\mathbb{H}_{\varepsilon, K, t}}^2 \\
&\leq \sum_{i=0}^{K-1} \left| \Psi(\delta\sqrt{\lambda_{i, \varepsilon}}) \right|^2 \left| \int_M \phi_{i, \varepsilon}(x')f_0(x')dV(x') \right|^2 \exp(\lambda_{i, \varepsilon}t) \\
&\leq \sum_{i=0}^{K-1} \left| \Psi(\delta\sqrt{\lambda_{i, \varepsilon}}) \right|^2 \left| \int_M \phi_{i, \varepsilon}(x')f_0(x')dV(x') \right|^2 \exp(2\lambda_{i, \varepsilon}t) \\
&\leq \exp(2\delta^{-2}t) \sum_{i=0}^{K-1} \left| \int_M \phi_{i, \varepsilon}(x')f_0(x')dV(x') \right|^2 \\
&\leq \text{vol}(M) \exp(2\delta^{-2}t) = \text{vol}(M) \exp\left(2\left(\frac{\gamma}{2C}\right)^{-\frac{2}{s}}t\right),
\end{aligned}$$

which finishes the claim. \square

To prove Theorem 5, we introduce the definition of the concentration function.

Definition 6. Fix $\varepsilon > 0$, $K \in \mathbb{N}$ and $t \in [0, 1]$. Consider the Gaussian Process $W_{\varepsilon, K}^t$ defined in (12). Let $S^t(\gamma) := -\log(\mathbb{P}(\|W_{\varepsilon, K}^t\|_\infty < \gamma))$. For any $f_0 \in \mathbb{H}_{\varepsilon, K}$, the concentration function of the Gaussian process $W_{\varepsilon, K}^t$ is defined as $\phi_{f_0}^t(\gamma) = \|f_0\|_{\mathbb{H}_{\varepsilon, K, t}}^2 + S^t(\gamma)$.

We have the following bound for the concentration function.

Lemma 3. Fix a sufficiently small $\varepsilon > 0$ and $K \in \mathbb{N}$. For $f_0 \in \mathbb{H}_{\varepsilon, K}$ with $\|f_0\|_\infty \leq 1$, we have

$$\|f_0\|_{\mathbb{H}_{\varepsilon, K, t}}^2 \leq \text{vol}(M) \exp\left(2C_3 K^{\frac{2}{d}} t\right), \quad S^t(\gamma) \leq C_6 K \log\left(\frac{C_7}{\gamma}\right),$$

where C_3 is the constant depending the volume of M used in Lemma 2, C_6 is a constant and C_7 depends on the volume of M .

Proof. By Proposition 5, we have $\|f_0\|_{\mathbb{H}_{\varepsilon, K, t}}^2 \leq \text{vol}(M) \exp(\lambda_{K-1, \varepsilon} t) \|f_0\|_\infty^2$. Based on Proposition 3 and Weyl's law in Lemma 2, when ε is sufficiently small, we have $\lambda_{K-1, \varepsilon} \leq 2\lambda_{K-1} \leq 2C_3 K^{\frac{2}{d}}$. Hence,

$$(18) \quad \|f_0\|_{\mathbb{H}_{\varepsilon, K, t}}^2 \leq \text{vol}(M) \exp\left(2C_3 K^{\frac{2}{d}} t\right) \|f_0\|_\infty^2 \leq \text{vol}(M) \exp\left(2C_3 K^{\frac{2}{d}} t\right).$$

For the second term, let $B_1^{\mathbb{H}_{\varepsilon, K, t}}$ be a unit ball centered at 0 in the $\mathbb{H}_{\varepsilon, K, t}$ norm. Let $N(\gamma, B_1^{\mathbb{H}_{\varepsilon, K, t}}, L^\infty)$ be the covering number of $B_1^{\mathbb{H}_{\varepsilon, K, t}}$ by balls of radius $\gamma > 0$ in the $L^\infty(M)$ norm. Clearly, $B_1^{\mathbb{H}_{\varepsilon, K, t}}$ can be covered by no more than $(\frac{4}{R})^K$ balls of radius $R > 0$ in the $\mathbb{H}_{\varepsilon, K, t}$ norm. By (18), if B_γ^∞ is a ball of radius $\gamma > 0$ centered at 0 in the $L^\infty(M)$ norm and if we set $R := \text{vol}(M) \exp\left(C_3 K^{\frac{2}{d}} t\right) \gamma$, then $B_R^{\mathbb{H}_{\varepsilon, K, t}} \subset B_\gamma^\infty$. Hence, $N(\gamma, B_1^{\mathbb{H}_{\varepsilon, K, t}}, L^\infty) \leq (\frac{4}{R})^K \leq \left(\frac{C_5}{\gamma}\right)^K \exp\left(-C_3 K^{\frac{2}{d} + 1} t\right) \leq \left(\frac{C_5}{\gamma}\right)^K$, where C_5 depends on the volume of M . Hence, $\log N(\gamma, B_1^{\mathbb{H}_{\varepsilon, K, t}}, L^\infty) \leq K \log\left(\frac{C_5}{\gamma}\right)$. With this bound, based on the same argument as that for [3, Proposition 3], we have $-\log(\mathbb{P}(\|W_{\varepsilon, K}^t\|_\infty < \gamma)) \leq C_6 K \log\left(\frac{C_7}{\gamma}\right)$, where C_6 is a constant and C_7 depends on $\text{vol}(M)$. The conclusion follows. \square

Let $\Phi(u) = \int_{-\infty}^u \frac{1}{\sqrt{2\pi}} e^{-\frac{w^2}{2}} dw$ be the cumulative density function (cdf) of the standard normal distribution. Then the following Lemma about $\Phi(u)$ can be found in [23]

Lemma 4. ([23, Lemma 4.10]) $\Phi(u)$ satisfies $\Phi(u) \leq \exp\left(-\frac{u^2}{2}\right)$ for $u < 0$. Moreover, we have $-\sqrt{2 \log\left(\frac{1}{v}\right)} \leq \Phi^{-1}(v)$ for $0 < v < 1$.

We introduce the following technical lemma to prove the main result of this section.

Lemma 5. If $\gamma_n = \left(\frac{n}{\log n}\right)^{-\frac{d}{2q+2d}}$ and n is sufficiently large so that $\log n \geq C_7$, then $\gamma_n^{-\frac{2q}{d}} \log\left(\frac{C_7}{\gamma_n}\right) \leq n\gamma_n^2$.

Proof. If $\log n \geq C_7$, then we have $\left(\frac{n}{\log n}\right)^{-\frac{d}{2q+2d}} \geq \left(\frac{n}{C_7}\right)^{-\frac{d}{2q+2d}}$. Hence, $\gamma_n \geq \left(\frac{n}{C_7}\right)^{-\frac{d}{2q+2d}}$, which is equivalent to $n \geq C_7 \gamma_n^{-\frac{2q+2d}{d}}$. Moreover, a straightforward calculation shows that $\gamma_n = \left(\frac{n}{\log n}\right)^{-\frac{d}{2q+2d}}$ is equivalent to $\gamma_n^{-\frac{2q}{d}} \log n = n\gamma_n^2$. Hence, $n\gamma_n^2 = \gamma_n^{-\frac{2q}{d}} \log n \geq \gamma_n^{-\frac{2q}{d}} \log\left(C_7 \gamma_n^{-\frac{2q+2d}{d}}\right) \geq \gamma_n^{-\frac{2q}{d}} \log\left(\frac{C_7}{\gamma_n}\right)$. \square

The main result of this section is summarized in the following proposition.

Proposition 7. Fix $\varepsilon > 0$. For the probability density function of \mathbf{T} , assume $p > 1$ and $q \geq \frac{d}{2}$. Take $f_0 \in \mathbb{H}_{\varepsilon, K}$ with $\|f_0\|_\infty \leq 1$. Denote $\gamma_n = \left(\frac{n}{\log n}\right)^{-\frac{d}{2q+2d}}$. Then, when ε is sufficiently small, n is sufficiently large and $\gamma_n \leq \frac{1}{K}$, we have

$$(19) \quad \mathbb{P}(\|W_{\varepsilon, K}^{\mathbf{T}} - f_0\|_\infty \leq \gamma_n) \geq \mathcal{A}_1 \exp(-\mathcal{A}_2 n \gamma_n^2),$$

where $\mathcal{A}_1 > 0$ and $\mathcal{A}_2 > 0$ are constants depending on $\text{vol}(M)$, and there is a Borel measurable subset $B_n \subset \mathbb{H}_{\varepsilon, K}$ such that

$$(20) \quad \mathbb{P}(W_{\varepsilon, K}^{\mathbf{T}} \notin B_n) \leq \exp(-C_6 n \gamma_n^2),$$

$$(21) \quad \log N(\tilde{\gamma}_n, B_n, L^\infty) \leq \frac{1}{4} n \tilde{\gamma}_n^2,$$

where $\tilde{\gamma}_n := 2\gamma_n$.

Theorem 5 follows from the above proposition and the same argument as Theorem 3.1 in [21].

Proof. We start by proving (19). Based on [22, Lemma 5.3], for a fixed $t \in (0, 1]$, we have

$$e^{-\phi_{f_0}^t(\gamma_n)} \leq \mathbb{P}(\|W_{\varepsilon, K}^{\mathbf{T}} - f_0\|_\infty \leq 2\gamma_n) \leq e^{-\phi_{f_0}^t(2\gamma_n)}.$$

Hence, $\mathbb{P}(\|W_{\varepsilon, K}^{\mathbf{T}} - f_0\|_\infty \leq 2\gamma_n) = \int_0^1 \mathbb{P}(\|W_{\varepsilon, K}^{\mathbf{T}} - f_0\|_\infty \leq 2\gamma_n) g(t) dt$

$$\geq \int_0^1 e^{-\phi_{f_0}^t(\gamma_n)} g(t) dt \geq \int_{t^*}^{2t^*} e^{-\phi_{f_0}^t(\gamma_n)} g(t) dt,$$

where $t^* \in (0, 1/2)$ will be determined. Since ε is sufficiently small, by Lemma 3,

$$\phi_{f_0}^t(\gamma_n) \leq \text{vol}(M) \exp\left(2C_3 K^{\frac{2}{d}} t\right) + C_6 K \log\left(\frac{C_7}{\gamma_n}\right) \leq \text{vol}(M) \exp\left(2C_3 \gamma_n^{-\frac{2}{d}} t\right) + C_6 \gamma_n^{-1} \log\left(\frac{C_7}{\gamma_n}\right),$$

where the second inequality holds by the assumption that $K \leq \frac{1}{\gamma_n}$. When n is sufficiently large, choose $t^* = \frac{1}{4C_3} (\gamma_n)^{\frac{2}{d}} \log\left(\frac{1}{\gamma_n}\right) \in (0, 1/2)$. Then, for $t \in [t^*, 2t^*]$, we have

$$\phi_{f_0}^t(\gamma_n) \leq \text{vol}(M) \exp\left(2C_3 \gamma_n^{-\frac{2}{d}} t\right) + C_6 \gamma_n^{-1} \log\left(\frac{C_7}{\gamma_n}\right) \leq \text{vol}(M) \gamma_n^{-1} + C_6 \gamma_n^{-1} \log\left(\frac{C_7}{\gamma_n}\right).$$

Hence, when n is sufficiently large, there is a constant $C_8 > 0$ depending on $\text{vol}(M)$ such that $\phi_{f_0}^t(\gamma_n) \leq C_8 \gamma_n^{-1} \log\left(\frac{C_7}{\gamma_n}\right)$. Observe that $t^* \rightarrow 0$ as $n \rightarrow \infty$ and the lower bound for $g(t)$, which is $\mathcal{C}_1 t^{-p} e^{-t^{-q}}$, goes to 0 as $t \rightarrow 0$. Therefore, $\inf_{t \in [t^*, 2t^*]} g(t) = \mathcal{C}_1 t^{*-p} e^{-t^{*-q}}$ when n is sufficiently large. As a result,

$$\begin{aligned} \mathbb{P}(\|W_{\varepsilon, K}^{\mathbf{T}} - f_0\|_\infty \leq 2\gamma_n) &\geq \int_{t^*}^{2t^*} e^{-\phi_{f_0}^t(\gamma_n)} g(t) dt \geq t^* \exp\left(-C_8 \gamma_n^{-1} \log\left(\frac{C_7}{\gamma_n}\right)\right) \mathcal{C}_1 t^{*-p} e^{-t^{*-q}} \\ &= \left(\frac{1}{4C_3}\right)^{1-p} \gamma_n^{\frac{2-2p}{d}} \log^{1-p}\left(\frac{1}{\gamma_n}\right) \exp\left(-C_8 \gamma_n^{-1} \log\left(\frac{C_7}{\gamma_n}\right) - (4C_3)^{-q} \gamma_n^{-\frac{2q}{d}} \log^{-q}\left(\frac{1}{\gamma_n}\right)\right). \end{aligned}$$

When n is sufficiently large, we have $(\gamma_n)^{-\frac{2}{d}} \log^{-1}\left(\frac{1}{\gamma_n}\right) > 1$. Using the assumptions that $p \geq 1$ and $q \geq \frac{d}{2}$, the above term is bounded below by $C_9 \exp\left(-C_{10} \gamma_n^{-\frac{2q}{d}} \log\left(\frac{C_7}{\gamma_n}\right)\right)$, where C_9 depends on the volume of M and p , C_{10} depends on the volume of M and q . Finally, by Lemma 5, when n is sufficiently large so that $\log n \geq C_7$, $\mathbb{P}(\|W_{\varepsilon, K}^{\mathbf{T}} - f_0\|_\infty \leq 2\gamma_n) \geq C_9 \exp(-C_{10} n \gamma_n^2)$. Hence, we obtain our claim (19)

$$\mathbb{P}(\|W_{\varepsilon, K}^{\mathbf{T}} - f_0\|_\infty \leq \gamma_n) \geq C_9 \exp(-4C_{10} n \gamma_n^2) = \mathcal{A}_1 \exp(-\mathcal{A}_2 n \gamma_n^2).$$

Second, we prove (20). Since $K \leq \frac{1}{\gamma_n}$, by Lemma 3, for any $t \in [0, 1]$,

$$S^t(\gamma_n) = -\log(\mathbb{P}(\|W_{\varepsilon,K}^t\|_\infty < \gamma_n)) \leq C_6 \gamma_n^{-1} \log\left(\frac{C_7}{\gamma_n}\right).$$

Let $B_1^{\mathbb{H}_{\varepsilon,K,0}}$ be the ball of radius 1 centered at 0 in $\mathbb{H}_{\varepsilon,K,0}$. Let B_1 be the unit ball centered at 0 in $L^\infty(M)$. Let $M = 2\sqrt{2C_6}\sqrt{n}\gamma_n$ and set $B_n := (MB_1^{\mathbb{H}_{\varepsilon,K,0}} + \gamma_n B_1) \cap \mathbb{H}_{\varepsilon,K}$. By Proposition 6, we have for $t \geq 0$

$$(MB_1^{\mathbb{H}_{\varepsilon,K,t}} + \gamma_n B_1) \cap \mathbb{H}_{\varepsilon,K} \subset (MB_1^{\mathbb{H}_{\varepsilon,K,0}} + \gamma_n B_1) \cap \mathbb{H}_{\varepsilon,K} = B_n.$$

Then, if we apply Borell's inequality, we have

$$\begin{aligned} \mathbb{P}(W_{\varepsilon,K}^t \notin B_n) &= \mathbb{P}(W_{\varepsilon,K}^t \notin (MB_1^{\mathbb{H}_{\varepsilon,K,0}} + \gamma_n B_1) \cap \mathbb{H}_{\varepsilon,K}) \leq \mathbb{P}(W_{\varepsilon,K}^t \notin (MB_1^{\mathbb{H}_{\varepsilon,K,t}} + \gamma_n B_1) \cap \mathbb{H}_{\varepsilon,K}) \\ &\leq 1 - \Phi(\Phi^{-1}(\exp(-S^t(\gamma_n))) + M) = \Phi(-\Phi^{-1}(\exp(-S^t(\gamma_n))) - M). \end{aligned}$$

Since $\mathbb{P}(\|W_{\varepsilon,K}^t\|_\infty < \gamma_n) \rightarrow 0$ as $\gamma_n \rightarrow 0$, if γ_n is small enough, we have $\mathbb{P}(\|W_{\varepsilon,K}^t\|_\infty < \gamma_n) < \frac{1}{4}$, and hence $\exp(-S^t(\gamma_n)) < \frac{1}{4}$. By Lemma 4, $\Phi^{-1}(\exp(-S^t(\gamma_n))) \geq -\sqrt{2S^t(\gamma_n)}$. So,

$$-\Phi^{-1}(\exp(-S^t(\gamma_n))) - M \leq \sqrt{2C_6\gamma_n^{-1} \log\left(\frac{C_7}{\gamma_n}\right)} - 2\sqrt{2C_6}\sqrt{n}\gamma_n.$$

By Lemma 5 and the fact that $q \geq \frac{d}{2}$, if $\gamma_n = \left(\frac{n}{\log n}\right)^{-\frac{d}{2q+2d}}$ and $\log n \geq C_7$, then we have

$$\gamma_n^{-1} \log\left(\frac{C_7}{\gamma_n}\right) \leq \gamma_n^{-\frac{2q}{d}} \log\left(\frac{C_7}{\gamma_n}\right) \leq n\gamma_n^2.$$

Hence, $-\Phi^{-1}(\exp(-S^t(\gamma_n))) - M \leq \sqrt{2C_6n\gamma_n^2} - 2\sqrt{2C_6}\sqrt{n}\gamma_n \leq -\sqrt{2C_6}\sqrt{n}\gamma_n$. By Lemma 4, $\mathbb{P}(W_{\varepsilon,K}^t \notin B_n) \leq \exp(-C_6n\gamma_n^2)$. Therefore, $\mathbb{P}(W_{\varepsilon,K}^t \notin B_n) \leq \int_0^1 \exp(-C_6n\gamma_n^2) g(t) dt \leq \exp(-C_6n\gamma_n^2)$.

Finally, we prove (21). Choose $\tilde{\gamma}_n = 2\gamma_n$. Then,

$$\log N(\tilde{\gamma}_n, (MB_1^{\mathbb{H}_{\varepsilon,K,0}} + \gamma_n B_1) \cap \mathbb{H}_{\varepsilon,K}, L^\infty) \leq \log N(\gamma_n, MB_1^{\mathbb{H}_{\varepsilon,K,0}}, L^\infty).$$

By Lemma 3 and the assumptions that $K \leq \frac{1}{\gamma_n}$ and $n \geq 8C_6$,

$$\log N(\gamma_n, MB_1^{\mathbb{H}_{\varepsilon,K,0}}, L^\infty) \leq K \log\left(\frac{C_7 M}{\gamma_n}\right) \leq \frac{1}{\gamma_n} \log(2\sqrt{2C_6}\sqrt{n}) = \frac{1}{2\gamma_n} \log(8C_6n) \leq \frac{1}{\gamma_n} \log n.$$

To show that $\frac{1}{\gamma_n} \log n \leq n\gamma_n^2$, it is equivalent to show that $\log n \leq n\gamma_n^3$. Since $\gamma_n = \left(\frac{n}{\log n}\right)^{-\frac{d}{2q+2d}}$, $n\gamma_n^3 = n^{1-\frac{3d}{2q+2d}} (\log n)^{\frac{3d}{2q+2d}}$. Hence, $\log n \leq n\gamma_n^3$ is equivalent to $(\log n)^{\frac{2q-d}{2q+2d}} \leq n^{\frac{2q-d}{2q+2d}}$, which follows from $q \geq \frac{d}{2}$ and $n \geq \log n$. In conclusion, we have $\log N(\tilde{\gamma}_n, B_M^{\mathbb{H}_t} + \gamma_n B_1, L^\infty) \leq n\gamma_n^2 = \frac{1}{4}n\tilde{\gamma}_n^2$. \square

DAVID B DUNSON, DEPARTMENT OF STATISTICAL SCIENCE, DUKE UNIVERSITY
Email address: dunsong@duke.edu

HAU-TIENG WU, DEPARTMENTS OF MATHEMATICS AND DEPARTMENT OF STATISTICAL SCIENCE, DUKE UNIVERSITY
Email address: hauwu@math.duke.edu

NAN WU, DEPARTMENT OF MATHEMATICS, DUKE UNIVERSITY
Email address: nan.wu@duke.edu